

# Novel Nondestructive Biosensors for the Food Industry

Hazal Turasan and Jozef Kokini

Department of Food Science, Purdue University, West Lafayette, Indiana 47907, USA;  
email: hazal.turasan@gmail.com, jkokini@purdue.edu

Annu. Rev. Food Sci. Technol. 2021. 12:539–66

The *Annual Review of Food Science and Technology* is  
online at [food.annualreviews.org](http://food.annualreviews.org)

<https://doi.org/10.1146/annurev-food-062520-082307>

Copyright © 2021 by Annual Reviews.  
All rights reserved

## Keywords

biosensors, food safety, food quality, optical, electrochemical, mechanical, RFID

## Abstract

An increasing number of foodborne outbreaks, growing consumer desire for healthier products, and surging numbers of food allergy cases necessitate strict handling and screening of foods at every step of the food supply chain. Current standard procedures for detecting food toxins, contaminants, allergens, and pathogens require costly analytical devices, skilled technicians, and long sample preparation times. These challenges can be overcome with the use of biosensors because they provide accurate, rapid, selective, qualitative, and quantitative detection of analytes. Their ease of use, low-cost production, portability, and nondestructive measurement techniques also enable on-site detection of analytes. For this reason, biosensors find many applications in food safety and quality assessments. The detection mechanisms of biosensors can be varied with the use of different transducers, such as optical, electrochemical, or mechanical. These options provide a more appropriate selection of the biosensors for the intended use. In this review, recent studies focusing on the fabrication of biosensors for food safety or food quality purposes are summarized. To differentiate the detection mechanisms, the review is divided into sections based on the transducer type used.

**ANNUAL  
REVIEWS CONNECT**

[www.annualreviews.org](http://www.annualreviews.org)

- Download figures
- Navigate cited references
- Keyword search
- Explore related articles
- Share via email or social media

# 1. INTRODUCTION

Biosensors are defined as analytical instruments that contain a biological sensing element or a biomimetic material, such as antibodies, nucleic acids, aptamers, enzymes, proteins, microorganisms, cells, or tissues, for quantitative or qualitative detection of target analytes (Morris 2013, Thakur & Ragavan 2013).

A typical biosensor is composed of a recognition element, transducer, detector, and display unit. The recognition elements can be either natural, such as enzymes from bacteria, nucleic acids, whole cells, antibodies, and biomolecular complexes like membranes, or artificially synthesized or modified materials, such as aptamers or molecularly imprinted polymers. On the basis of these recognition elements, biosensors can be classified as, e.g., aptamer based, nucleic acid based, antibody based, or enzyme based (Chambers et al. 2008). In a different approach, biosensors are also classified according to the working principle of the transducer. The transducer is the element where the information obtained from the recognition element, such as the degree of binding of an analyte, the end product of a reaction, or the changing structure, is converted into a readable or measurable signal. The types of transducers generally used in biosensors are electrochemical transducers that measure changing electrical output, optical transducers that measure light output or absorbance, thermal transducers that measure heat output, piezoelectric transducers that measure mass change, or acoustic transducers that measure specific sound outputs (Chambers et al. 2008). Each biosensor type has subcategories based on the type of signal read; for example, electrochemical sensors can be categorized as amperometric biosensors, potentiometric biosensors, conductometric biosensors, etc. (Figure 1). In this review, the most commonly used biosensor types in the food industry are discussed.

The main aim of a biosensor is to provide information about the concentration of a specific analyte. For a biosensor to be considered successful and to be comparable to lab-scale analytical devices, it must possess other properties (Thakur & Ragavan 2013). Most importantly, a biosensor has to show an accurate linear response to the target analyte concentration and needs to be sensitive enough to measure low to very low concentrations of the analyte, especially if the analyte is found at low concentrations in foods or the disease/toxicity causing threshold concentration is low.

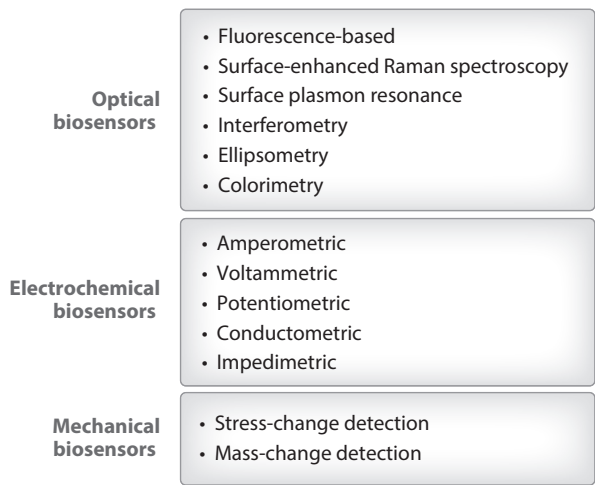


Figure 1

Classification of biosensors based on detection mechanisms and types of transducers used.

A biosensor also must be selective for the target analyte and should not be affected by the complex composition and structure of the tested sample or other compounds with similar structures to the target analyte. Antibodies and aptamers usually provide this kind of specificity. Stability, shelf life, and ability to give reproducible signals over a long period of time are other important properties of a successful biosensor (Thakur & Ragavan 2013). Lastly, a biosensor has to make rapid measurements with minimal sample preparation, especially because one of the most desirable applications of biosensors is on-site measurements, where there are usually limited tools to prepare samples.

## 2. BIOSENSORS IN THE FOOD INDUSTRY

The applications of biosensors in the food industry are gaining a great deal of importance because of the increasing frequency of foodborne outbreaks and incidents (Kumar et al. 2012). Also, increasing health consciousness requires the production of foods without certain undesirable ingredients, such as allergens or natural contaminants. This requires a detailed screening of food products in each step of handling, processing, storage, distribution, and transportation (Thakur & Ragavan 2013). However, currently, the standard methods include the use of expensive lab-scale analytical devices, such as high-performance liquid chromatography (HPLC) or gas chromatography–mass spectrometry, trained personnel, and long analysis times to obtain reliable results (Dridi et al. 2017). Biosensors serve as powerful alternative measurement techniques with their rapidity, portability, ease of use, and nondestructive nature. They are particularly needed in the food industry for food safety, quality, and authenticity (Bunney et al. 2017). Food safety biosensors focus on the detection of unwanted harmful food contaminants, such as toxins, food pathogens, spoilage microorganisms, and allergens. Food quality biosensors measure nutritional content, freshness, appearance, or smell as well as other quality parameters. Biosensors for authenticity usually confirm the origin of the foods and search for adulteration or counterfeiting (Bunney et al. 2017). In this review, studies focusing on the fabrication of food biosensors are reviewed on the basis of the type of transducer used. However, in each section a wide range of applications are included to give the reader a broad view of all the areas biosensors are used in the food industry.

### 2.1. Optical Biosensors

Optical biosensors, also referred to as optodes, use optical transducers such as interferometers, resonators, gratings, and refractometers (Damborský et al. 2016, Thakur & Ragavan 2013). When the target analyte is captured, a luminescent process such as electrochemiluminescence or optical diffraction occurs, and the resulting light intensity is measured as the output signal (Girigoswami & Akhtar 2019). In some cases, the emitted light is visible to the naked eyes, such as a simple color change. Spectroscopic techniques such as Raman spectroscopy or fluorescence spectroscopy may be required to capture the intensity of the signal. Optical biosensors can make both label-based and label-free detections. In label-free detections, the signal is generated when the analyte directly interacts with the transducer. In label-based detections, the use of a label, such as fluorescent quantum dots (QDs) or fluorescent dyes, is required to generate a signal upon analyte–label interaction (Estrela et al. 2016).

Food safety optical biosensors are frequently used in the food industry. For example, food toxins, allergens, and contaminants are detected and quantified (Gezer et al. 2016b,c). High specificity and sensitivity, label-free detection options, nondestructive detection mechanisms, and the possibility of remote detection of harmful chemicals or pathogens make optical biosensors advantageous over conventional methods and other biosensors (Narsaiah et al. 2012).

Optical biosensors can be classified in different groups based on detection principles. These classifications include surface-enhanced Raman scattering, fluorescence, interferometry, ellipsometry, surface plasmon resonance, colorimetry, and others (Girigoswami & Akhtar 2019). In this section, recent studies that used the most commonly employed optical biosensor types for food safety are discussed and summarized.

**2.1.1. Surface-enhanced Raman spectroscopy biosensors.** Surface-enhanced Raman spectroscopy (SERS) uses the enhanced Raman scattering of target analyte molecules when they are in the vicinity of SERS-active surfaces, such as nanostructured metals (Lal et al. 2008), which provide strong plasmonic fields due to their high electron densities when the incident laser is shone onto their surface. These regions of high plasmonic activity are called hot spots, and they are usually stronger around the crevices in metallic nanostructures than on flat metallic surfaces (Maher 2012). This is why a great majority of the SERS studies focus on fabricating novel nanostructured metallic SERS-active materials to increase the number of hot spots (Jia et al. 2019, Ma et al. 2020, Turasan et al. 2019). When molecules of interest fall within the hot spots, their Raman signal is enhanced (by up to  $10^{10-13}$  orders of magnitude), which enables very low limits of detection (LODs) and sometimes even single-molecule detection.

There are two mechanisms proposed for SERS signal enhancement. The first is the electromagnetic mechanism, which is due to the presence of enhanced electromagnetic fields localized within a few nanometers of nanostructured metallic surfaces formed by surface plasmon resonances. The charge transfer mechanism results from resonant charge transfer effects between a molecule chemically adsorbed onto the surface and the metal itself (Maher 2012, Wu et al. 2012).

Detection of pesticides in agriculture has become a very important application area of SERS biosensors. The rapidity of the SERS technique as well as the availability of handheld Raman detectors enable detection of pesticides on-site with minimal sample preparation. Thiabendazole, a fungicide used for various fruits and vegetables, is detected using a simple surface swab technique coupled with SERS (He et al. 2014). Methanolic thiabendazole solutions with concentrations ranging between 0.01 and 100  $\mu\text{g/mL}$  were prepared and thiabendazole molecules were conjugated with silver dendrites through silver-sulfur bonds to enhance the Raman signal. Using the calibration curve prepared from the thiabendazole solutions, the LOD was calculated as 0.01  $\mu\text{g/mL}$ . Swab tests were conducted on apple samples that were presoaked in thiabendazole solutions and the final accuracy of the swab-SERS method was between 89.2% and 115.4%, resulting in high reliability for such a rapid fungicide detection method.

Another harmful fruit and vegetable insecticide, acetamiprid, was also detected from spiked solutions, the surface of apples, and apple juice, using the same surface swab technique and silver dendrites (Wijaya et al. 2014). The calibration curve prepared from the SERS measurements of spiked acetamiprid solutions yielded an LOD of 0.5  $\mu\text{g/mL}$ . Samples collected off the contaminated apple surfaces with swabs yielded an LOD of 0.125  $\mu\text{g/cm}^2$ . Store-bought apple juice samples were also spiked with acetamiprid and SERS measurement gave an LOD of 3  $\mu\text{g/mL}$ .

Both of these studies focused on detecting pesticides without any specific target-binding agents and therefore lack selectivity against the target analyte. SERS detection of four different pesticides, with aptamers specific to the four tested pesticides, was used to provide selectivity (Pang et al. 2014). Aptamers were conjugated to the silver dendrites using the thiol (sulfur) linkage (Figure 2). The empty surfaces remaining on the silver dendrites were then conjugated with 6-mercaptohexanol to eliminate nonspecific binding of other molecules or dendrite-to-dendrite binding. The modified aptamers were then tested on the pesticides, isocarbophos, omethoate, phorate, and profenofos, both separately and as a mixture. Each pesticide gave unique peak formations in SERS spectra, which enabled differentiation of detected pesticides when a mixture

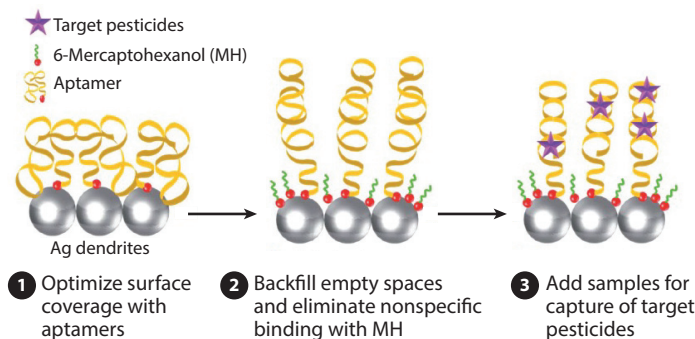


**Figure 2**

Surface modification of silver dendrites with aptamers for the detection of pesticides. Adapted from Pang et al. (2014) with permission from the Royal Society of Chemistry.

of all four pesticides was used. The selectivity of the sensor was confirmed against acetamiprid. LODs for each pesticide were calculated as  $0.4 \mu\text{M}$ ,  $3.5 \mu\text{M}$ ,  $24 \mu\text{M}$ , and  $14 \mu\text{M}$  for phorate, isocarbophos, omethoate, and profenofos, respectively. Apple juice was successfully tested as a real food model to detect pesticides.

SERS studies shown above required a sample preparation period during which the target analyte is collected, dissolved in a solvent, and conjugated with the metallic nanoparticles. A different and more novel SERS technique was developed in which the target analyte can be measured in real-time and in situ directly from the sample itself without lengthy sample preparation (Yang et al. 2016). Two pesticides, ferbam and thiabendazole, were detected directly from the surface of spinach leaves after a direct deposition of gold nanoparticles on the surface of the leaves. The LODs for ferbam and thiabendazole were calculated to be  $1 \mu\text{g/L}$  and  $2 \mu\text{g/L}$ , respectively. A comparison of thiabendazole LODs calculated with this method and the surface swab method shows that the direct measurement method is 10 times more sensitive than the surface swab method (He et al. 2014). Ferbam, which is a nonsystemic pesticide, penetrated at least  $100 \mu\text{m}$  into the spinach leaves when the leaves were not washed (Yang et al. 2016). However,  $\text{NaHCO}_3$  washing prevented ferbam penetration into the leaves. Thiabendazole, which is a systemic pesticide, penetrated through the leaves even after the leaves were washed (**Figure 3**). In nonwashed leaves, penetration depth was higher than in washed samples. These results show that the SERS mapping technique applied directly to the metallic nanoparticle deposited on food surfaces is an effective way to determine penetration depths of pesticides.

Silver dendrites were also used in the detection of ricin, which is a protein toxin naturally produced in castor beans and a bioterrorism agent (He et al. 2011). Selective detection of ricin B was done by using aptamers, and spiked orange juice and milk were tested as real food samples. SERS spectra of the spiked solutions showed the formation of two new peaks at  $985$  and  $621 \text{ cm}^{-1}$  wavenumbers, which proved the capture of ricin B using the dendrites. The LOD was  $10 \text{ ng/mL}$ , but a linear correlation could not be obtained because the distance aptamers created between the silver dendrites and the captured ricin molecules exceeded the distance required for optimum SERS enhancement and therefore a sensitive measurement could not be done. This method, however, was successful as a yes/no sensor that detects the existence of the ricin molecules. The lowest concentrations of ricin B detected in orange juice and milk were  $50 \text{ ng/mL}$  and  $100 \text{ ng/mL}$ , respectively.

In a parallel study of the same group, a single DNA aptamer for the ricin B chain was fabricated using the SELEX method, which was capable of capturing the entire ricin toxin not just the ricin B

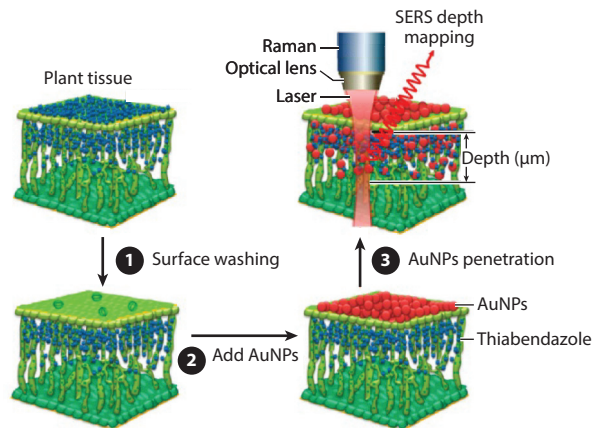


**Figure 3**

Detection mechanism of thiabendazole from the surface of washed spinach leaves with surface-enhanced Raman spectroscopy (SERS) mapping technique. The numbers show the necessary steps for gold nanoparticle (AuNPs) penetration for direct sample measurement with SERS. Reprinted with permission from Yang et al. (2016); copyright (2016) American Chemical Society.

subsection (Lamont et al. 2011). This aptamer (SSRA1) was also conjugated onto silver dendrites for SERS detection. Ricin was successfully detected from various liquid foods, including apple juice, orange juice, lemonade, and 2% milk, and the detection was not affected by the different pH values of these samples. The lowest concentration of ricin detected from complex food samples was 30 ng/mL, which is lower than the concentration commercial ELISA kits can detect and lower than the previous ricin B SERS sensor could detect (He et al. 2011).

There are other SERS active surfaces used in the detection of food contaminants, allergens, and toxins in the literature. For example, Klarite™, a commercially available gold-coated silicon wafer with a patterned square lattice area, was used to detect melamine, a chemical adulterant found in milk or pet foods (Lin et al. 2008). The Klarite™ SERS active platform was also used to detect spores of five *Bacillus* strains: *B. cereus* ATCC 13061, *B. cereus* ATCC 10876, *B. cereus* sp., *B. subtilis* sp., and *B. stearothermophilus* sp., using dipicolinic acid as the biomarker (He et al. 2008). SERS analysis was successful in detecting a single bacteria spore. *Bacillus* strains could be differentiated because of the slight differences, originating from different quantities and distribution of sporal components, in their SERS signatures.

Bimetallic nanostructures can lower LODs for food toxins. Bimetallic gold core–silver satellite nanostars allowed detection of aflatoxin B1 in picogram levels (Li et al. 2016). Silver nanoparticles (satellites) were conjugated with aflatoxin B1 aptamers, and gold nanostars were conjugated with other complementary aptamers. In the presence of aflatoxin B1, the aflatoxin aptamer–conjugated silver nanoparticles released the gold nanostars and preferred attachment to the aflatoxins. When a higher aflatoxin B1 was introduced to the system, more gold core–silver satellite assemblies were disassembled and the SERS intensity was reduced. A linear intensity decrease was observed in the range of 1–1,000 pg/mL aflatoxin B1, and the LOD was calculated as 0.48 pg/mL. The selectivity of the system was tested and validated against seven other biotoxins. The applicability of this new design was tested with spiked peanut milk and percent recovery was between 88% and 103%, indicating successful aflatoxin detection in real food samples.

Other important studies focused on fabricating environmentally friendly biodegradable SERS platforms for the detection of food toxins. Gezer et al. (2016a) developed a soft lithography



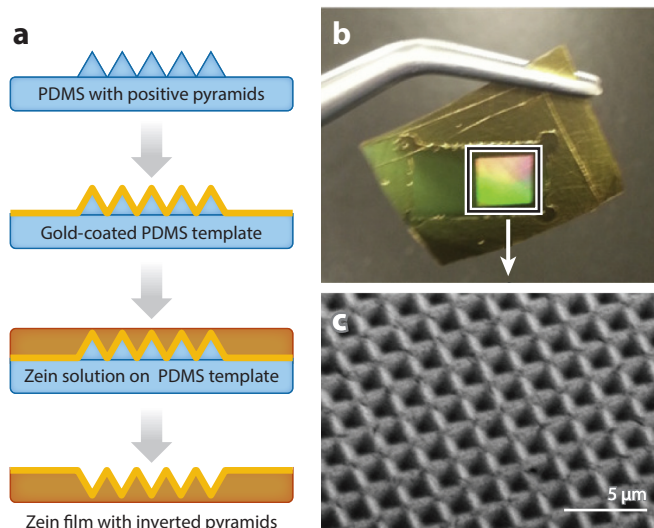


**Figure 4**

(a) Schematic of the fabrication process for zein-SERS sensors. Polydimethylsiloxane (PDMS) with positive pyramid structures were used as a template. After being coated with gold by an e-beam evaporator, zein solution is poured. Following the drying in a desiccator at room temperature, zein films are peeled off to provide inverted pyramid structures with a gold coating. (b) Macroscopic image of zein-SERS sensor on gold-coated side. Squared area shows the location of the nanophotonic patterns. (c) Scanning electron microscopy images of the inverted pyramid structures. Adapted from Gezer et al. (2016b) with permission from Elsevier.

method to fabricate zein-based SERS platforms with inverted nanopyramid photonic structures (**Figure 4**). Polydimethylsiloxane (PDMS) molds with positive nanopyramid structures were coated with a 200-nm-thick gold layer. Ethanolic zein solutions were then cast on PDMS molds and, after drying, the zein films were peeled off the surface, with the gold layer completely transferred onto the zein films because of its higher affinity to zein.

The resulting gold-coated zein films with inverted nanopyramid structures showed a SERS enhancement factor of  $10^4$ . These zein film-based SERS platforms were then successfully used in the detection of a food carcinogen, acrylamide (Gezer et al. 2016b), and the most common peanut allergen, Ara h1 (Gezer et al. 2016c). For the detection of acrylamide, aqueous solutions of acrylamide were directly deposited on the surfaces of zein-SERS platforms and the LOD was calculated as 10 μg/mL. For Ara h1 detection, the surfaces of zein platforms were modified with antibodies and the spectra were analyzed with principal component analysis (PCA). The LOD was 0.14 mg/mL. In a follow-up study, chemical cross-linking with 4% glutaraldehyde was found to significantly improve the nanostructure transfer fidelity from PDMS molds to zein films (Barber et al. 2019).

Decorating the surface of the gold-coated zein nanophotonic platforms with gold nanoparticles increased the SERS enhancement factor by almost three times because of the increased number of hot spots (Jia et al. 2019). Gold-nanoparticle-decorated gold-coated zein-SERS platforms were also tested for the detection of pyocyanin, a toxin secreted by *Pseudomonas aeruginosa*, and the LOD was calculated as 25 μM. Among gold, silver, and silver-coated gold bimetallic nanoparticles, decorating the surface of the gold-coated zein platforms with silver-coated gold nanoparticles gave the highest SERS enhancement factor,  $3.4 \times 10^5$  (Ma et al. 2020).

Electrospun zein nanofiber mats were tested as an alternative biodegradable SERS platform for detecting food toxins (Turasan et al. 2019). The high surface area of zein nanofibers enabled a high level of gold nanoparticle decoration and hot-spot formation on the surface of fibers. Crosslinking zein nanofibers helped prevent gold colloid solution from spreading on the fiber mat and increased the SERS enhancement factor to  $10^6$ . Decorating the zein nanofiber mats with silver-coated gold nanoparticles instead of gold nanoparticles gave an even higher SERS enhancement factor ( $2.5 \times 10^6$ ). This higher SERS enhancement factor reduced the limit of acrylamide detection to 1.15 ng/mL. This detection limit is lower than the FDA's standard limit of quantitation (LOQ) for acrylamide in food products (10 ng/mL) (FDA 2020).

**2.1.2. Fluorescence-based biosensors.** Fluorescence-based biosensors are also widely used optical biosensors in foods. The detection mechanism is based on fluorescence, and the electromagnetic excitation of the molecule is done with a high-energy light and the emission occurs at a lower energy (Girigoswami & Akhtar 2019, Grimm et al. 2013). The molecules that can display fluorescence (fluorophores or fluorochromes) show characteristic absorption and emission spectra (Girigoswami & Akhtar 2019). The most commonly used fluorescent dyes in imaging technologies are fluorescein, rhodamine, Coumarin, Cy3, and Thioflavin T, and their selection in applications is usually done based on their quantum yield (Grimm et al. 2013). QDs have emerged as a powerful type of fluorophores in the past decade. They are 1–12-nm-sized luminescent semiconducting nanocrystals such as cadmium selenide (CdSe) nanocrystals, and their emission wavelength is directly proportional to their sizes (Bonilla et al. 2016, Lobnik et al. 2012). Compared to fluorescent dyes, QDs have wider absorption spectra, higher molar absorbances, narrower emission spectra, higher photostability, a longer lifetime at the excited state, and higher quantum yields, which make them far superior to fluorescent dyes (Sozer & Kokini 2014).

Fluorescence-based biosensors are nondestructive, and they provide high imaging resolution with the ability of real-time monitoring of analytes. These advantages have made fluorescence-based biosensors popular in the detection of food components and contaminants (Girigoswami & Akhtar 2019, Sharma et al. 2018).

A switch-on fluorescent biosensor was developed for the detection of the antioxidant glutathione in food samples (Xu et al. 2015). A graphitic carbon nitride QD was used as the fluorescent probe and the initial fluorescence of these QDs was quenched (fluorescence intensity reduced) with  $Hg^{2+}$  ions, which were electrostatically attracted to the negatively charged surface of the QDs. In the presence of glutathione,  $Hg^{2+}$  ions were captured by glutathione molecules and the QDs were freed from  $Hg^{2+}$  ions, gaining their fluorescence intensity back and becoming switched-on. Fluorescent intensity was proportional to glutathione concentrations, and an LOD of 37 nM was achieved. Real food samples, including tomatoes, grapes, cucumbers, and spinach, were tested and recoveries were above 94% for all the samples. For patulin mycotoxin detection, the same fluorescence quenching principle was used (Bagheri et al. 2018). A silver nanoparticle/zinc metal organic framework (Ag/ZnMOF) composite was used to catalyze the reaction between terephthalic acid and  $H_2O_2$  forming the fluorescent probe 2-hydroxy terephthalic acid (HTA). In the presence of patulin mycotoxin molecules, the catalytic activity of Ag/ZnMOFs was quenched, reducing the rate of HTA formation and fluorescence intensity. A linear correlation between patulin concentration and intensity decrease was observed, and the LOD was calculated as 0.06  $\mu\text{mol/L}$ .

The mycotoxin zearalenone, which is commonly found in cereals and cereal-based products such as corn, wheat, oat, barley, soybeans, and beer, is also highly toxic to humans. Highly fluorescent upconversion nanoparticles (UCNPs) conjugated with zearalenone aptamers were used as fluorescent probes (Wu et al. 2017). UCNPs are another class of luminescent probes that can



combine two or more low-energy photons and generate a single high-energy photon by an anti-Stokes process (Han et al. 2014). As the zearalenone concentration increased, aptamers preferred binding to zearalenone molecules, linearly decreasing the fluorescence intensity of the UCNP complex. Spiked corn and beer samples were tested, and LODs were calculated as 0.126  $\mu\text{g/kg}$  and 0.007  $\mu\text{g/L}$ , respectively. UCNP were also used in the detection of *Escherichia coli* (Li et al. 2020). *E. coli* aptamers were conjugated with magnetic nanoparticles and cDNA–UCNPs to form a fluorescent probe complex. As the *E. coli* was added to the solutions with increasing concentration, the aptamers selectively bound to *E. coli* cells, reducing the fluorescent intensity of UCNP complexes. Within the added *E. coli* concentration of 58 cfu/mL to  $58 \times 10^6$  cfu/mL, a linear correlation between the *E. coli* levels and decreasing fluorescent intensity was found. The sensor was tested with *Staphylococcus aureus* and *Salmonella typhimurium* species as well, and the selectivity against *E. coli* was confirmed (Li et al. 2020). The UCNP-based fluorescent sensor was tested in pork meat spiked at different concentrations of *E. coli*, and recovery rates were above 97%, showing the successful performance of the sensor. UCNP biosensor arrays were also used to identify a total of seven pathogenic food bacteria, *E. coli*, *S. aureus*, *Salmonella*, *Listeria monocytogenes*, *Cronobacter sakazakii*, *Shigella flexneri*, and *Vibrio parahaemolyticus* (Yin et al. 2020). The fabricated biosensor array had very high accuracy in identifying each species when they were tested separately or in blends. Tap water, milk, and beef were tested as real food samples with 92% accuracy.

An organophosphorus pesticide, diazinon, was detected with another upconversion fluorescence biosensor, where the fluorescence intensity of UCNP was recovered in the presence of pesticide molecules (Wang et al. 2019). An LOD of 0.05 ng/mL was achieved and detection in real food samples (tap water, lake water, apple, pear, and tea powder) was successfully done, with recoveries above 90%. To detect the herbicide glyphosate, a conjugation of two QDs was used, mercaptopropionic acid–capped cadmium telluride (CdTe) QDs and carbon QDs synthesized from chitosan (Bera & Mohapatra 2020). The fluorescence of CdTe QDs was quenched in the presence of carbon QDs, and when glyphosate was added, the CdTe QDs/carbon QD complex disintegrated and fluorescence intensity increased. An LOD of 2 pM was achieved and real food samples (ginger, capsicum, and cucumber) were tested successfully.

A different application of QDs focused on identification and distribution of proteins in dough structures. In this assembly of studies, QDs have been proved to be superior imaging probes for cereal proteins compared to organic dyes (Sozer & Kokini 2014). The distribution of gliadins, which are the alcohol-soluble proteins of wheat that contribute to the gluten network in wheat doughs, were imaged using antibody-conjugated QDs during different times of dough mixing (Bozkurt et al. 2014). The same antibody-conjugated QDs were also successfully used to image gliadin proteins in baked food products (Ansari et al. 2015). In the following studies, separate antibodies were developed for high- and low-molecular-weight subunits of glutenins and conjugated to QDs for imaging the distribution of gliadins and glutenins separately in hard, soft, and semolina wheat doughs (Bonilla et al. 2018, 2019a, 2020a,b). The roles of each gluten-forming protein in wheat dough formation were separately identified during different stages of mixing (Bonilla et al. 2019b).

**2.1.3. Colorimetric biosensors.** Colorimetric biosensors are commonly used to detect food toxins and assess food quality and are low cost, easy to use, and able to do real-time monitoring. Their main principle is to measure color change qualitatively or quantitatively upon the capture of the analyte molecules, which trigger a reaction that leads to the color change (Ebralizde et al. 2019). This change is often visible to the naked eye, but an image analysis or spectroscopic methods might be required for subtle changes. In food applications, the color change is usually observed based on either a physical property change, like temperature or pH, or the formation

of new conjugates, such as chemical binding of analytes to antibodies. The freshness of trout fish samples was analyzed using a colorimetric biosensor using a pH reactive dye, alizarin, which was encapsulated in zein nanofiber mats (Aghaei et al. 2020). As the fish spoiled, the pH changed and the electrospun fiber mats changed their colors because of their alizarin core. These nanofiber mats were used as indicators on the packaging material. The freshness of milk was also detected using pH-sensitive color-changing biosensor discs (Weston et al. 2020). The agarose discs were fabricated from polydiacetylene/zinc oxide (ZnO) conjugates, which dissociated as the milk spoiled and lactic acid production increased the acidity, leading to a color transition from blue to red.

Zhang et al. (2020) developed a different type of colorimetric biosensor to detect antioxidants. The 3,3',5,5'-tetramethylbenzidine (TMB) color probe was oxidized with metal ions to obtain a blue color, and different antioxidants were then introduced into the system, reversing the oxidation reaction and leading to the fading of the blue color. By measuring the absorbance of antioxidant-added solutions, eight different antioxidants were successfully discriminated and quantitatively detected. The color-changing property of TMB probes was also successfully used in the detection of five pesticides (Zhu et al. 2020). Blue color formation of TMBs with  $H_2O_2$  was first catalyzed using graphene-based nanozymes, which are nanomaterials with intrinsic enzyme-like characteristics. In the presence of pesticides, the catalytic activity of nanozymes was reduced, and the reaction between TMB and  $H_2O_2$  was slowed down, leading to a fading blue color.

A more complex colorimetric biosensor design was used to detect *E. coli* O157:H7 (Ren et al. 2019). Bacteria cells were captured on a lateral flow strip by antibody-modified gold nanoparticle probes. Branched polyethylenimine-loaded liposomes were then conjugated to the gold nanoparticle probes. When a gold nanoparticle/phosphate-buffered saline with Tween® 20 (PBST) mixture was poured over the strip, PBST destroyed the liposomes, releasing polyethylenimine molecules, which caused aggregation of gold nanoparticles leading to a red color on the strips, which indicated successful detection of *E. coli*. Tests done on spiked cranberry juice samples showed an LOD of 100 cfu/mL. The same concept of red color formation upon gold nanoparticle aggregation was also used in the fabrication of another colorimetric biosensor for detecting 26 sulfonamides in honey (Chen et al. 2017). These paper strip-based sensors were successful in detecting sulfonamides with LODs between 0.25 and 25  $\mu\text{g/kg}$ . There are many other examples of antibody-based strip colorimetric sensors (immunochromatographic strip sensors) for the detection of food contaminants (Chen et al. 2014, Lin et al. 2020).

## 2.2. Electrochemical Biosensors

Electrochemical biosensors might be the most commonly used biosensors because of their simplicity and the wide application possibilities. They use electrochemical transducers that detect either a chemical reaction or binding of a chemical to a recognition element on the surface of the electrodes and convert these into an electrical signal to be read by the detector. Electrical cells are used for measurements, which usually consist of a working and a reference electrode and an optional platinum wire auxiliary electrode (Ronkainen et al. 2010). The reference electrode, which is usually made of Ag/AgCl, is located away from the reaction zone to maintain a known potential (Grieshaber et al. 2008). The working electrode, also referred to as the redox electrode, is where the electrochemical reaction occurs (Grieshaber et al. 2008). The optional auxiliary electrode is used to pass the charge from electrolysis and protect the reference electrode (Ronkainen et al. 2010).

Electrochemical biosensors can be (a) biocatalytic devices, where a cell, a tissue, or an enzyme produces an electroactive material in the presence of the target analyte, or (b) affinity sensors, where the target analyte molecules are captured by recognition elements on the surface of the

electrodes (Ronkainen et al. 2010). However, electrochemical biosensors are usually categorized on the basis of the detected electrical property: amperometric, voltammetric, potentiometric, conductometric, or impedimetric (**Figure 1**). Both amperometric and voltammetric biosensors measure the current produced in the working electrode as a response to an applied potential; however, in amperometry the voltage is set to a specific value and in voltammetry a potential range is scanned (Ronkainen et al. 2010). Potentiometric biosensors measure the charge potential accumulation when no current flows (Grieshaber et al. 2008). Conductometric biosensors test the current-conducting ability of the analyte between electrodes and are sometimes considered a subgroup of impedimetric biosensors, which measure resistive and capacitive properties of materials when their equilibrium state is disturbed by an alternating current (AC) in a range of frequencies (Grieshaber et al. 2008, Guan et al. 2004).

Electrochemical biosensors are widely employed because they are inexpensive, easy to construct and use, and portable (Ronkainen et al. 2010). They do not require large amounts of samples, and by reducing the size of the electrodes, the signal-to-noise ratio can be increased, which allows lower LODs, even at atto- ( $10^{-18}$ ) or zeptomolar ( $10^{-21}$ ) levels (Grieshaber et al. 2008, Ronkainen et al. 2010). Also, the detection ability of electrochemical biosensors is not affected by the presence of other components, such as chromophores or fluorophores, which allows measurements of turbid samples. This also becomes advantageous in the analysis of food samples, which often requires analyzing complex structures that include proteins and fat molecules.

In this section, the most commonly used electrochemical biosensor types in food science and technology are included, and recent studies using these techniques are summarized. Electronic-nose (e-nose) biosensors are also included in this section because they find many applications in food science and industry.

**2.2.1. Amperometric/voltammetric biosensors.** The principle in amperometric/voltammetric biosensors is measuring the changing current in the electrodes, which is due to the oxidation/reduction of the end product of the reaction, such as  $H_2O_2$  formation or oxygen depletion as the reaction occurs (Claussen et al. 2009, Misun et al. 2016). Although the changing current is sometimes directly correlated to the analyte concentration, in some studies, the inhibition of the reaction is an indicator of the compound.

Amperometric biosensors are used in the detection of food adulteration. Melamine, which is a food adulterant used to increase the apparent protein content of milk products, has been detected by micellar electrokinetic capillary chromatography with a three-electrode amperometric sensor (Wang et al. 2010). Capillary electrophoresis was used as an analytical separation technique, and a carbon-disc working electrode was placed at the end of a capillary outlet to measure the oxidation current created by melamine. An LOD of  $2.1 \times 10^{-6}$  g/mL was achieved, and testing spiked milk and infant formula samples provided recovery rates over 83%. A disposable enzyme-based amperometric biosensor was developed to detect paraoxon-ethyl pesticide from spinach samples (Hua et al. 2019). The inhibitory effect of paraoxon-ethyl on the enzyme acetylcholinesterase (AChE) was used as the detection mechanism, and the presence of pesticide molecules inversely affected the AChE-catalyzed hydrolysis reaction of acetylthiocholine. The AChE enzyme was immobilized on the working electrode, and the changing current was used to calculate the degree of inhibition and estimate the pesticide concentration. An LOD of 0.03  $\mu$ g/L was achieved, and the spiked spinach test results showed a very good correlation with the HPLC results.

Tria et al. (2016) developed a microlithographically fabricated electrochemical cell-on-a-chip biosensor that allows both amperometric and luminescence-based detection of the carcinogenic ochratoxin A. A synthetic peptide, NFO4, was immobilized on the surface of a working electrode that had a high binding affinity toward ochratoxin A molecules and acted as a biorecognition

element. For simultaneous chemiluminescent measurements, ochratoxin A was also conjugated with horseradish peroxidase (HRP), which catalyzed a reaction that emits light in the presence of  $\text{H}_2\text{O}_2$ /luminol. The biosensor was successful in detecting ochratoxin A both amperometrically and chemiluminescently. An antibody-based amperometric biosensor was developed for detecting another class of mycotoxins, zearalenones (Liu et al. 2017). Before modifying the surface with antibodies, the glassy carbon working electrode was modified with polyethylenimine-functionalized multiwalled carbon nanotubes and gold and platinum nanoparticles to increase the surface area of the electrode and capture more mycotoxin molecules. At a constant voltage of 0.18 V, an LOD of 1.5 pg/mL was achieved. Also, the use of antibodies provided good selectivity of zearalenones in the presence of other mycotoxins.

Food freshness measurements were also conducted with amperometric biosensors. Henao-Escobar et al. (2016) fabricated a dual enzymatic amperometric biosensor for simultaneous detection of histamine and putrescine, two biogenic amines indicating food spoilage. A two-working-electrode array was fabricated on the system, one functionalized with histamine dehydrogenase for detecting histamine and the other functionalized with putrescine oxidase to detect putrescine. LODs for histamine and putrescine were 8 and 10  $\mu\text{M}$ , respectively. The dual biosensor was tested in fresh octopus and red wine samples, and the results showed good correlation with HPLC measurements. In a similar study, a tyrosinase enzyme-based amperometric biosensor was developed to detect tyramine, another biogenic amine that indicates spoilage in fermented food products (da Silva et al. 2019). A much lower LOD, 0.71  $\mu\text{M}$ , was achieved. Four fermented food products (yogurt, Roquefort cheese, red wine, and beer) were successfully tested and showed recovery rates higher than 93%. Bacterial contamination of milk samples was also tested with an amperometric biosensor, where acyl-homoserine lactones (AHLs) were detected as indicators of *Pseudomonas aeruginosa* contamination (Özcan et al. 2020). 2,2,6,6-tetramethyl-1 piperidinyloxy zinc(II) phthalocyanine radical groups functionalized on the surface of the electrodes were used as the biomimetic receptor molecules for AHLs. An LOD of  $1.8 \times 10^{-6}$  mol/L was achieved for spiked solutions. In real milk samples, a slightly higher LOD of  $3.7 \times 10^{-6}$  mol/L was found.

Amperometric biosensors can also be used to measure the antioxidant content of foods. A xanthine oxidase enzyme-based amperometric biosensor enabled detection of antioxidants in various fruit samples, where the enzyme catalyzed a reaction between hypoxanthine and uric acid, leading to the formation of either  $\text{H}_2\text{O}_2$  or  $\text{O}_2$  radicals (Becker et al. 2019). Antioxidant presence reduced the  $\text{H}_2\text{O}_2$  and  $\text{O}_2$  radicals and decreased the measured current at the electrodes. The biosensor achieved an LOD of 2.17  $\mu\text{mol/L}$ . Gallic acid was successfully detected in strawberry, orange, passion fruit, and pulp of Amazonian fruits.

A nylon membrane-based amperometric biosensor with an LOD of 0.2  $\mu\text{M}$  was used to detect polyphenolic compounds in tea, alcoholic beverages, and water samples using a polyphenol oxidase enzyme obtained from bananas (Narang et al. 2011). Mohtar et al. (2019) also developed an amperometric biosensor to detect polyphenols in propolis samples with a slightly higher LOD of 0.83  $\mu\text{M}$ , where the detection of polyphenols was achieved via the oxidation ability of a laccase enzyme immobilized on the electrodes.

An enzyme-based amperometric biosensor was used to classify red, white, and rosé wines on the basis of their carboxylic acid levels (Milovanovic et al. 2019). A three-sensing-channelled sensor was designed, and each channel was functionalized with a different enzyme, i.e., lactate oxidase, fumarase, or sarcosine oxidase, to detect L-lactate, tartrate, or general carboxylic acid levels, respectively, using  $\text{H}_2\text{O}_2$  formation rates. PCA and self-organized maps were successfully used to differentiate and classify the data collected from 31 types of wine. Ethanol contents of alcoholic beverages were also detected with an alcohol oxide functionalized amperometric

biosensor (Soylomez et al. 2019). A 4,7-di(thiophen-2-yl)benzo[c][1,2,5]selenadiazole-co1H-pyrrole-3-carboxylic acid-coated graphite electrode was used to sense ethanol amounts with an LOD of 0.052 mM. Measurements on rum, vodka, and raki showed comparable results to the labeled values on the products.

Some studies focused on fabricating greener amperometric biosensors. Low-cost nitrogen-doped graphene-like mesoporous nanosheets were synthesized from okara, the biomass waste of soybean processes, and used to functionalize the glassy carbon working electrode of the biosensor to detect vitamin C (Sha et al. 2019). The nanosheets provided a lower overpotential and a lower LOD (0.51  $\mu$ M) compared to carbon nanotube functionalized glassy carbon electrodes (7.59  $\mu$ M) or nonfunctionalized glassy carbon electrodes (51.8  $\mu$ M). Vitamin C recovery rates calculated from real beverages showed recovery rates above 96%. Rouf et al. (2020) used another biopolymer, corn protein zein, to capture antibodies onto the working electrode for the detection of the common food allergen gliadin, which causes celiac disease. The addition of three nanocomposites, carbon nanotubes, Laponite®, and graphene oxide, to the zein layer was tested, and the carbon nanotube-loaded zein coating provided the highest electrochemical signal. The antibodies anchored to zein layers successfully detected gliadin molecules with an LOD of 0.5 ppm using cyclic voltammetry and had an excellent specificity against other food toxins.

**2.2.2. Potentiometric biosensors.** In potentiometric biosensors, the charge accumulation between the electrodes is measured. A greater voltage change from the initial equilibrium state indicates larger biosensor activity. Use of potentiometric biosensors is not as common as amperometric biosensors in food science and technology, possibly because of their high sensitivity to the environment and temperature and their time-consuming nature (Luka et al. 2015).

In an earlier study, a light-addressable potentiometric sensor (LAPS) was developed to detect *E. coli* from rucola, lettuce, carrots, and mixed salad samples (Ercole et al. 2003). pH variations occurring because of  $\text{NH}_3$  production of a urase-*E. coli* antibody conjugate were used as an *E. coli* presence indicator. 10 cells/mL were successfully detected and when compared to conventional cfu counting methods, the biosensor was 10–20 times faster in delivering accurate results. In a more recent application, *E. coli* O157:H7 DNA was used as the indicator, and the detection was done using ZnO nanorod arrays functionalized on the surface of the LAPS chip (Tian et al. 2019). The lowest detected *E. coli* DNA corresponded to 100 cfu/mL of *E. coli* O157:H7. A disposable paper-based potentiometric immunosensor was developed for detecting *S. typhimurium*, where the paper strip was integrated with a poly(3,4-ethylenedioxythiophene) polystyrene sulfonate (PEDOT:PSS) conductive polymer-coated filter paper to act as an internal solution reservoir (Silva et al. 2019). The binding of bacteria cells to the antibodies conjugated to the surface of the immunosensor disrupted the flux of internal solution and shifted the potential. Thus, greater potential shifts were correlated to a higher number of bacteria cells. An LOD of 5 cells/mL was achieved. However, during *Salmonella* detection in a real apple juice sample, only a 54% recovery rate was achieved, suggesting there is still room for improvement for this biosensor.

For the detection of a water-pollutant herbicide, diquat, a screen-printed potentiometric sensor was fabricated using PEDOT as a solid contact material on the platforms for selective detection of diquat molecules (Kamel et al. 2020). Aqueous diquat solutions were tested, and increasing concentrations linearly shifted the measured potential with an LOD of 0.026  $\mu$ g/mL. Potato samples spiked with diquat were tested as real food samples, and the results obtained with the potentiometric biosensor were not significantly different than results obtained with the HPLC method and showed high accuracy.

A contact hybrid potentiometric method sensor was fabricated with a screen-printed electrode pair coated by a MFAS-OS-2 membrane. This sensor was used to detect vitamin C activity in

various fruits and vegetables either on-site or in situ (Brainina et al. 2020). The system included screen-printed electrodes, working and reference electrodes, and a  $[\text{Fe}(\text{CN})_6]^{3-/4-}$  mediator impregnated membrane, which allows testing of either a vitamin C-loaded membrane in situ or a slice of food sample on-site. The recovery rates of tested vitamin C solutions with the membrane were above 96%, and for the food samples of garlic, beet, tomato, peach, pear, cucumber, melon, apple, pumpkin, plum, and carrot, the recovery rates were above 92%. However, the use of this biosensor on very juicy fruits like oranges and lemons was found unsuitable because the juice diluted the mediator system in the membrane.

**2.2.3. Impedimetric biosensors.** In electrochemical impedance spectroscopy (EIS), a sinusoidal AC voltage is applied and two types of current response are measured: in-phase current, which determines the resistive component of impedance, and out-of-phase current, which determines the capacitance component of impedance (Suni 2008). The applied AC voltage is usually small (2–10 mV) so that it can obtain a linear response. To interpret the EIS results, the data are first fitted to equivalent circuit models with resistors and capacitors, then the Nyquist plots are drawn from these circuits, which provide a visual assessment of the changing dynamics in the system.

Of all the electrochemical biosensor types, impedance biosensors are considered the best option for conducting a label-free detection because in EIS, the interaction between the target analyte molecules and the recognition elements can be measured directly on the surface of the transducer, without the need for using a label such as fluorophores, active enzymes, or magnetic beads (Malvano et al. 2020). The basic label-free detection diagram with EIS biosensors is shown in **Figure 5**, and the resulting Nyquist plot shows the changing system dynamic with the analyte capture. Another advantage of EIS biosensors is their insensitivity against environmental disturbances, which makes them extra advantageous in detecting food components (Suni 2008).

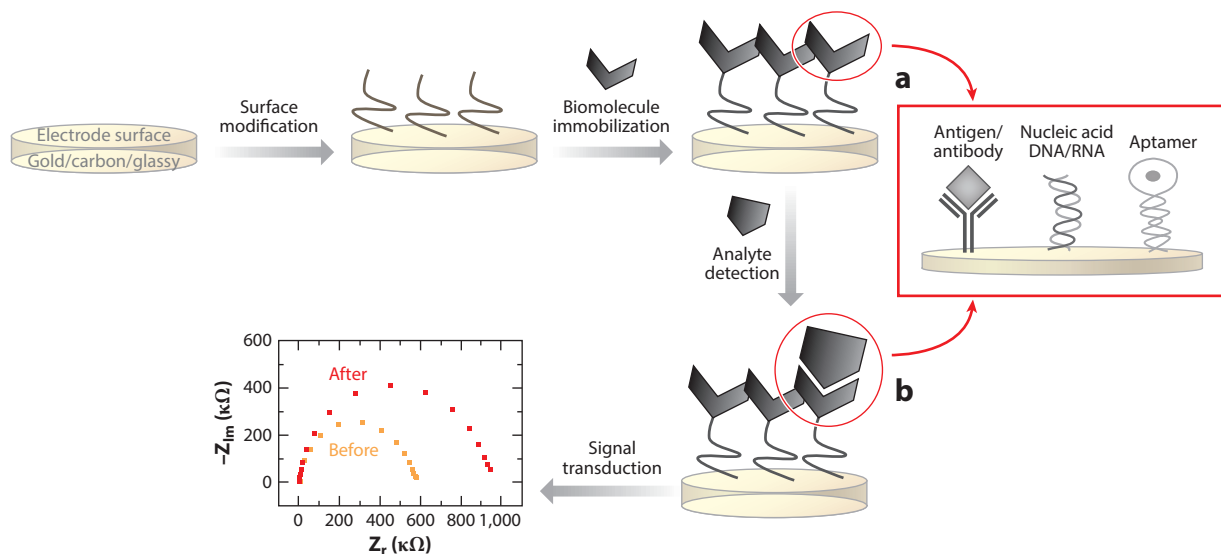


**Figure 5**

Schematic explaining the label-free impedimetric biosensors. (a) Recognition elements. (b) Label-free detection of target analyte. Adapted from Malvano et al. (2020) with permission of Taylor & Francis Group.



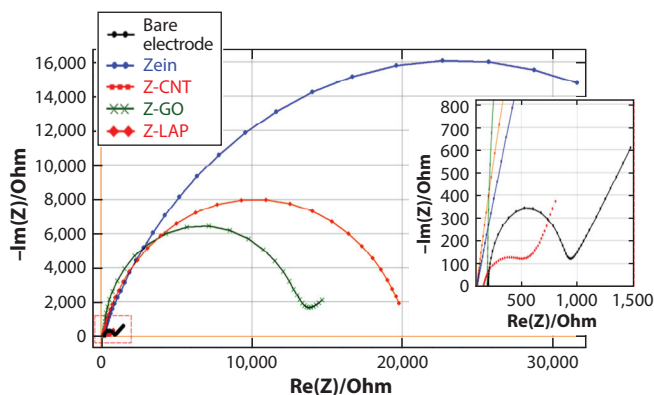


**Figure 6**

Nyquist plots for bare electrode, zein-coated (Z), zein-laponite-coated (Z-LAP), zein-graphene-oxide-coated (Z-GO), and zein-carbon-nanotube-coated (Z-CNT) electrodes. Adapted from Rouf et al. (2020) with permission from Elsevier.

One of the most common uses of EIS is for characterization of the biosensor fabrication process. EIS methods can be used in combination with other electrochemical techniques. For example, in a study in which donkey meat adulteration in cooked sausage samples was investigated, the EIS technique was used to characterize the fabrication of a locked nucleic acid (LNA) based electrochemical genosensor (Mansouri et al. 2020). After each step of electrode surface modification, impedance of the system was measured and the circle diameters in the Nyquist plot were compared. When the bare gold electrode was initially functionalized with the single-stranded DNA (ssLNA) capture probes, the resistance went up from 105 to 134  $\Omega$ , making the initial circle in the plot larger. After incubation with mercaptohexanol, the nonspecifically bound capture probes were eliminated, reducing the resistance to 111  $\Omega$ . Lastly, when the target DNA molecules were captured by the probes, the resistance went up to 277  $\Omega$ , indicating successful binding. EIS results were also compared to linear sweep voltammetry results for confirmation of successful biosensor fabrication. In Rouf et al.'s (2020) study, the selection of nanocomposites, which are added to the zein layer covering the surface of working electrodes, was done based on EIS results. Bare electrode resistance was compared to those of the pristine zein layer and the zein-laponite, zein graphene oxide, and zein-carbon nanotube (Z-CNT) composite layers, and the lowest resistance was obtained with the Z-CNT layer (**Figure 6**). A Z-CNT layer-coated working electrode was then used for the detection of gliadin using cyclic voltammetry.

Aghoutane et al. (2020) used EIS for both characterization of their biosensor and calculation of their LOD. They fabricated a molecular-imprinted, polymer-based, screen-printed gold electrode for detecting malathion (MAL), an organophosphorus insecticide, in olive fruits and oils. They compared the resistances of a bare gold electrode with those of a MAL/polymer-coated electrode and a final electrode after the MAL was extracted from the polymer blend and confirmed successful preparation of the sensor. Later, EIS was used to measure the retention ability of different MAL concentrations and the LOD was calculated as 4.6 pg/mL.

In another study in which the EIS technique was used for both biosensor characterization and detection, gliadin was detected from real food samples with the use of aptamers (Malvano et al. 2017). The concentrations of the gliadin aptamer and the cross-linker (polyamidoamine) used to link the aptamers to the surface of the transducer were optimized on the basis of their impedance, and the analytical performance was then tested with EIS, where the LOD was 5  $\mu\text{g/L}$ . Gliadin

content detected in lager beer, gluten-free beer, gluten-free bread, corn flour, and rice samples showed good correlation with ELISA results. Another food allergen, Ara h1, which is the peanut allergen, was detected using a DNA-based impedimetric biosensor (Sun et al. 2012). A stem-loop probe, where in the absence of the target DNA the system is closed and in the presence of the target DNA it is open, was designed for detection of Ara h1. The LOD was 0.35 fM and peanut milk analysis results gave a concentration of  $3.2 \times 10^{-13}$  mol/L, suggesting excellent applicability in real food samples. Other applications of EIS biosensors in food science include detection of mycotoxins (Khan et al. 2019), aflatoxins (Yagati et al. 2018), metal ions (Kaur et al. 2020), and noroviruses (Baek et al. 2020).

**2.2.4. Electronic-nose biosensors.** The e-nose concept was first introduced in 1982 (Herrero et al. 2016, Liu et al. 2020, Persaud & Dodd 1982), and it has since been used frequently in food quality assessment. In later studies, e-noses were defined as “an instrument, which comprises an array of electro-chemical sensors with partial specificity and an appropriate pattern-recognition system, capable of recognizing simple or complex odors” (Gardner & Bartlett 1994, p. 213; Herrero et al. 2016). The array of chemical sensors is often fabricated using micro-electro-mechanical-systems technology and consists of gas sensors that measure the volatile compounds. Even though the design of each e-nose may be different, e-noses typically have gas sensor arrays that adsorb the odor molecules, signal conditioning circuits, air and electronic control units, data processing software, and a pattern recognition unit that can do quantitative and qualitative data measurements (Herrero et al. 2016, Xu et al. 2016). E-noses offer many advantages, including real-time monitoring, rapidity, nondestructive testing, low-cost, portability, and high accuracy in testing. Because of these advantages and practicality, many researchers focus on fabricating e-nose sensors for testing foods.

One of the most common applications of e-noses is to test the freshness of food products. For example, Jia et al. (2020) developed a predictive model to test salmon fillet freshness using an e-nose system with PCA and radial basis function neural networks (RBFNNs). An e-nose with 18 gas sensors that measure different volatile compounds, including ammonia, amines, hydrocarbons, solvents, and aromatics, was used to test the effects of different storage temperatures on salmon spoilage. The e-nose/PCA-RBFNN model system was successful in predicting the freshness of salmon fillets (within 15% relative error). The freshness of meat products (beef, chicken, and fish) was predicted using a metal-oxide-semiconductor sensor (MOS)-based e-nose that has seven different gas sensors (hydrocarbons, methane, ethanol, hydrogen sensors) combined with the Hidden Markov Model (HMM) for discrimination and quantitative detection (Liu et al. 2020). In freshness evaluation results, high sensitivity and high selectivity values were observed (>96%) for all three types of meats.

Oil oxidation is another parameter that affects oil quality. Nine types of edible oils (olive, peanut, soybean, rapeseed, camellia, corn, sunflower, linseed, and walnut) were tested with an e-nose to understand the degree of oxidation (Xu et al. 2016). The e-nose had 10 MOS-based gas sensors, and data analysis was conducted using cluster analysis, PCA, and linear discriminant analysis. The e-nose had good selectivity and sensitivity, and all three analysis methods showed recognition rates higher than 96%.

Another e-nose with 12 sensors was used to detect fungi infections on a freeze-dried edible mushroom, *Agaricus bisporus* (Wang et al. 2020). The mushrooms were contaminated with five different fungi, *Aspergillus niger*, *Aspergillus flavus*, *Penicillium chrysogenum*, *Aspergillus fumigatus*, and *Aspergillus ochraceus*, and the gas collected at the headspace of infected mushroom samples was used for analysis. E-nose data analyzed with PCA and partial least squares discriminant analysis were also compared to near-infrared (NIR) and mid-infrared (MIR) spectroscopic results. The

discrimination accuracy of the e-nose method (97%) was comparable to NIR (99%) and MIR (97%) spectroscopies.

Beer aromas were also detected and predicted with a portable e-nose that had nine different gas sensors (Gonzalez Viejo et al. 2020). Two artificial neural network models were used to predict the aromas, both of which were highly accurate. The analysis of variance (ANOVA) results between each sensor also showed that e-nose successfully differentiated the beer aromas. Another MOS-based e-nose (Agrinose) was used to assess wheat-bread quality during four days of storage by using the volatile compounds forming during staling and the loss of aroma (Rusinek et al. 2020). Data were analyzed with PCA, and the results showed that the Agrinose was successful in diagnosing bread staling during storage.

### 2.3. Mechanical Biosensors

Mechanical biosensors have been successfully fabricated more recently (Boisen et al. 2011). Often also referred to as nanocantilever-based biosensors, mechanical biosensors have many advantages because of their nano- or microsizes. They are label-free, portable, highly accurate, low-cost, and fast. Also, because the detectable target mass is proportional to the mass of the device itself, when mechanical biosensors are fabricated at nanoscales, very small mass resolutions and therefore low LODs (zeptogram scales) can be achieved (Arlett et al. 2011, Boisen et al. 2011). The smaller size of the cantilevers also increases their mechanical compliance, which enables force detections as low as pN levels (Arlett et al. 2011).

On the basis of their detection mechanisms, mechanical sensors are usually classified into two categories: sensors that detect surface stress change and sensors that detect mass change (Figure 1) (Bashir 2004). In surface stress-detecting sensors, target analyte molecules that are binding to the surface of the cantilevers cause a change in the surface stress of the cantilever, which leads to a quasistatic deflection at the very tip of the cantilever. Thus, the capture of the analytes is determined from the deflection of the cantilever. Other parameters such as humidity or temperature changes can also cause a bulk stress change on the cantilever if the cantilever is made of materials that are responsive to these parameters (Boisen et al. 2011). These bulk stress changes, for instance, can occur when an exothermic chemical reaction takes place on the cantilever upon target molecule capture and the dissipated energy changes the deflection of the cantilever. In the second type of mechanical biosensors, which are also referred to as dynamic-mode mechanical sensors, landing of the target analyte molecules on the surface of the cantilevers increases the mass leading to a drop in the oscillation resonance frequency of the cantilever (Arlett et al. 2011). Thus, by using the difference between the resonance frequency before and after capture of the analyte, the mass of the molecules on the cantilever can be calculated. Smaller cantilever dimensions usually lead to increasing resonance frequencies; therefore, smaller mass changes (at atto or femtogram scales) can be measured with smaller geometries (Boisen et al. 2011). In mass change-detecting mechanical sensors, the position of the molecules on the cantilever often plays an important role because molecules closer to the tip of the cantilevers often affect the resonance frequency more than the molecules away from the tip of the cantilevers. Applications of mechanical biosensors in food science include cell and bacteria detection, pesticide and drug detection, and, sometimes, food quality assessments.

A mass-based mechanical sensor with a silicon cantilever was used to detect *Listeria innocua* bacteria and bovine serum albumin (BSA) protein (Gupta et al. 2004). To observe the smallest number of *L. innocua* cells that can be detected with the silicon cantilever, a nonspecific binding detection was applied in which the cantilever was directly inoculated with the bacterial cells and the resonance frequency before and after inoculation was measured using a Doppler vibrometer

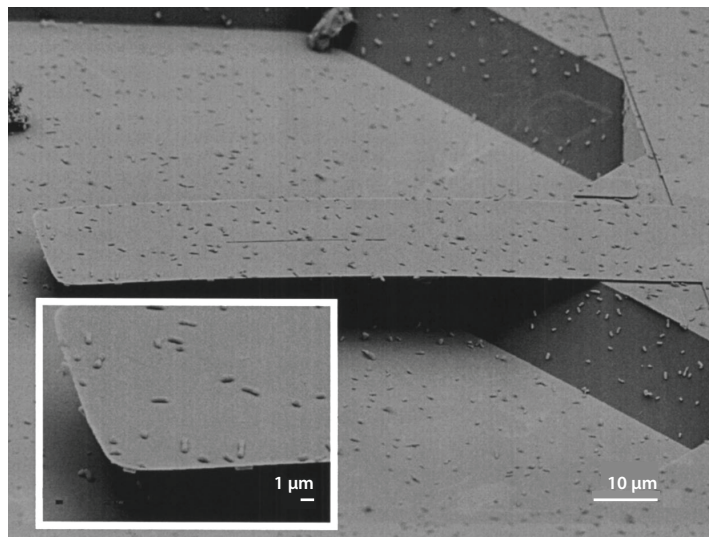


**Figure 7**

Scanning electron microscope micrographs showing nonspecific binding of *Listeria innocua* bacterial cells to cantilever and surrounding area of sample. Inset: Higher magnification view showing the individual bacterial cells. Adapted from Gupta et al. (2004) with permission from the American Institute of Physics Publishing.

(Figure 7). A total number of 180 cells caused a frequency change of almost 1 kHz and a single cell weight could be estimated to be 85 fg from the measurements, which is very close to the actual weight of a single *L. innocua* cell (79 fg). The frequency measurements after BSA adsorption to the surface also showed that the mass of the protein coating can be successfully detected. Specific *L. innocua* detection was also conducted by decorating the surface with antibodies, and the weight of the antibodies was also taken into account. A 500-Hz change in resonance frequency indicated the binding of 62 bacteria cells in total when antibodies were used. *L. innocua* was also detected more recently with another cantilever-based biosensor in which polymer microcantilevers were fabricated onto the end of standard single-mode fibers (ferrule-top optical cantilever sensor) (Li et al. 2018). Bacteria cells were captured using antibodies, and the detections were carried out measuring the deflection of the cantilever (bending of the cantilever downward) at the nanometer scale with increasing inoculated bacteria concentrations. Concentrations of less than  $10^5$  cfu/mL were successfully detected within 30 mins.

The silicon-based cantilevers developed by Gupta et al. (2004) were used in the fabrication of a device with microfluidic channels and in the detection of HeLa cells (Park et al. 2008). An array of cantilevers was constructed in a microfluidic channel device and the cells were injected and adhered to the cantilevers. After a 3-day incubation period, the resonance frequencies of the cantilevers were measured to estimate the mass of the cells. The frequency changes recorded for cell growth media without cells (2.93 kHz) and cell media with HeLa cells (5.43 kHz) indicated 1-ng and 3.6-ng mass changes, respectively. The mass of a single HeLa cell was successfully calculated from the frequency shifts and validated by comparing it to the actual weight of the cells.

*Vibrio cholerae*, which is the pathogenic bacteria that produces the cholera disease-causing toxin, has been detected with a microcantilever sensor (Khemthongcharoen et al. 2015). The microcantilever was fabricated with a polysilicon wire in it, which acted as a piezoresistive material to detect the length of the deflection upon target capture. To detect the bacteria, the surface of the microcantilever was modified with 3-mercaptopropionic acid and a DNA probe that binds to the *ctxA*

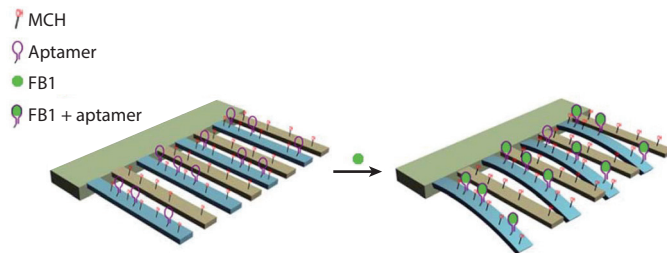


**Figure 8**

Illustration of microcantilever modification and detection of fumonisin B-1 (FB1). The sensing cantilevers were modified with aptamer self-assembled monolayers (SAMs) to bind with FB1. Meanwhile, the reference cantilevers were coated with 6-mercapto-1-hexanol (MCH) SAMs. The binding of FB1 induced the sensing cantilevers to bend downward compared to reference cantilevers. Adapted from Chen et al. (2015) with permission from the Royal Society of Chemistry.

gene of *V. cholerae*. The detection sensitivity of this microcantilever-based sensor was 3.25 pg of DNA template. Also, detection of *V. cholerae* was done in a real food sample, contaminated fresh shrimp meat, and 835 cells/g could be detected. When this microcantilever sensor was coupled with a PCR (polymerase chain reaction) method as an enrichment process for the *ctxA* gene, this detection limit was brought down to 0.835 cells/g.

Fumonisin B-1 (FB-1), which is a group of mycotoxins produced by molds found in cereal food products and especially corn, has been detected using a microcantilever array biosensor (Chen et al. 2015). In the design of the array, cantilevers that are designed to capture FB-1 were modified with FB-1 specific aptamers and those that served as control cantilevers were modified with 6-mercapto-1-hexanol to eliminate nonspecific binding (**Figure 8**). A range of FB-1 concentrations was tested (0.1–40 µg/mL), and the deflection lengths were calculated for each concentration. A linear correlation between the deflection amplitudes and the concentrations was obtained with an LOD of 33 ng/mL.

A new design of cantilever-based mechanical biosensors was developed for detecting organophosphorus pesticides (Cai et al. 2019). Microcantilevers were fabricated with built-in electrothermal resonance excitation and Wheatstone piezoresistive signal readout elements. The surface of the cantilevers was covered with Parylene-C, a polymer used in the fabrication of these elements as well as to protect these elements from the corrosive analytes, and a reservoir was created at the free tip of the cantilever for sample introduction. Frequency shifts were recorded as the dimethyl methylphosphonate (DMMP), an organophosphorus simulant, was injected into the reservoir. The microcantilevers with this new design successfully detected the DMMP molecules with an LOD of 5 ppb.

In another study, a quartz crystal mass-based biosensor was developed for the detection of an antiviral drug, amantadine, in animal-sourced food products (Yun et al. 2019). The surface of the crystal was first decorated with 11-mercaptoundecanoic acid and then a conjugate of amantadine-bovine serum albumin was linked to 11-mercaptoundecanoic acid molecules using ethyl(dimethylaminopropyl) carbodiimide/*N*-hydroxysuccinimide (EDC/NHS) cross-linking. The frequency shifts were measured as the amantadine antibodies were subjected to the surface of the crystal because a conjugation between the amantadine molecules and the antibodies increased the weight on the surface of the crystal. An LOD of 1.3 ng/mL was achieved. Tests on four different spiked animal-based food products, chicken muscle, duck muscle, egg, and pork, showed recovery percentages above 83% and similar detection levels to HPLC-MS/MS results.

In a similar study, meat products were analyzed for their freshness using a cantilever-based mechanical biosensor (Costa et al. 2020). Cadaverine levels, a biogenic amine that increases as meats are spoiled, were used as a freshness indicator, and a binding agent, cyclam, was used to bind the cadaverine molecules to the surface of the cantilevers. The resonance frequency of the cantilevers was measured to calculate the mass of the captured cadaverine molecules. Cadaverine binding rate calculations between different meat products showed that fish had the fastest cadaverine production, followed by chicken, beef, and pork, during a 3-day measurement period.

## 2.4. RFID-Based Biosensors

Radio frequency identification (RFID)-based biosensors are another type of sensors used in food applications, especially in the food production and transportation stages of food handling. In this technology, radio frequencies are used for identifying an object; therefore, RFID sensors are categorized as wireless sensor technologies (Ruiz-Garcia et al. 2009).

An RFID system consists of three main components: an RFID tag (also referred to as transponder), a tag reader (also referred to as RFID interrogator or antenna), and the main computer, which contains the database (Costa et al. 2013, Ruiz-Garcia et al. 2009). The RFID tag is the component that is attached to the product to be identified and consists of a microchip that stores the data and an antenna that receives the radio waves emitted by the tag reader. The RFID tag powers the microchip by converting the radio waves into electricity and transmits the data back to the tag reader (Kumar et al. 2009). Depending on the power source, an RFID tag could be an active tag, a passive tag, or a semipassive tag. Active tags contain batteries that allow them to activate the microchip themselves and transmit the data to the tag readers; therefore, they have the strongest signals. Passive tags need the tag reader's power to activate the microchip and transmit the data back to the reader; thus, passive tags work only when the reader is in the proximity of the tags. Even though passive tags give weaker signals compared to active tags, they are the most commonly used type of tags in the food industry because of their very low cost (Kumar et al. 2009). Semipassive tags have a battery to activate the microchip but still need the tag reader to transmit the data back. The RFID tag reader is the device that powers the tags by converting electricity into radio frequencies and receives the identification data back from the tag. In the food supply chain, handheld tag readers are typically used for convenience and on-site identification.

The main applications of RFID-based biosensors in the food industry are to maintain good traceability of the food products through the food supply chain and usually to monitor environmental factors like temperature or humidity (Costa et al. 2013, Kumar et al. 2009). Additionally, smart food packages can now be fabricated with RFID technology for the detection of food spoilage and food quality. One great advantage of RFID-based sensors is their rapidity. Unlike most of the optical or electrochemical biosensors, RFID-type detection does not require device setups and/or other spectroscopic techniques. Simply by reading the tags, data can be collected in a few seconds, which resembles barcode reading. This is probably why RFID-based sensors have become very popular with real-life applications in the food industry. However, this technique is still not as common as barcode reading due to the comparably higher cost of fabricating RFID tags.

Tao et al. (2012) showed the fabrication of a silk-based RFID food sensor that can be easily adhered to the food material's curved surface without deformation and is safe to be used on food products because of the edible nature of silk. The silk acts as the carrier for gold antennas of the sensor and provides a glue-like adhesiveness when it is plasticized/softened by moisture, which makes it easy to stick directly on food surfaces such as eggs, tomatoes, meat, and apples. The RFID sensors were first used to test banana ripening. During storage, the physical (color, texture,



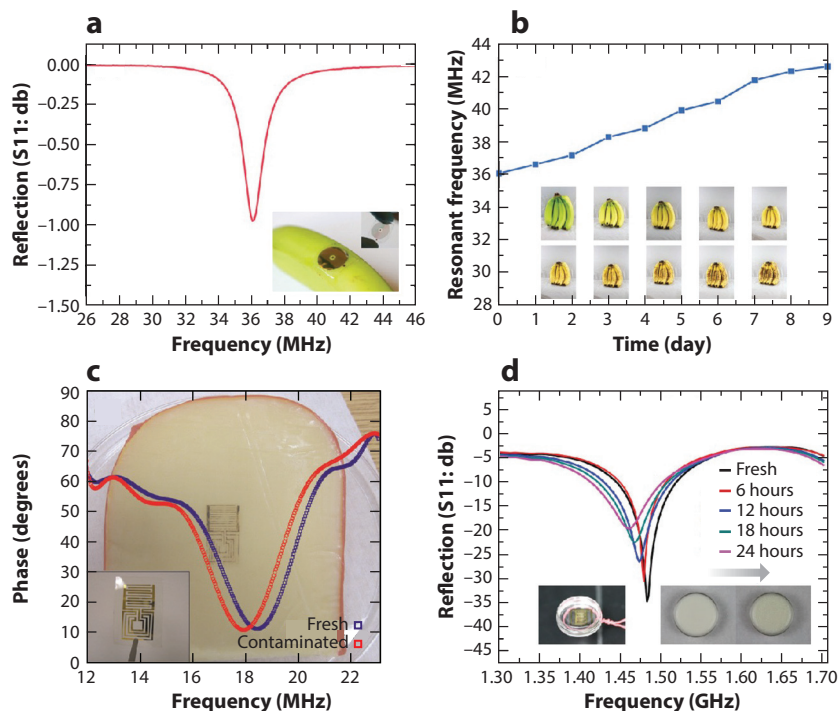


**Figure 9**

(a) Experimentally measured reflection spectra of a silk RFID-like antenna attached to a banana. (b) Experimentally measured time-dependent resonant frequencies of the silk antenna while the banana ripened over 9 days. (c) Experimentally measured frequency-dependent impedance phase angle of a silk sensor applied to a slice of cheese to detect bacterial contamination. (d) Experimentally measured frequency responses of a silk sensor attached to a plastic container filled with milk during spoilage. Adapted from Tao et al. (2012) with permission from John Wiley and Sons. Abbreviation: RFID, radio frequency identification.

firmness) and chemical (ethylene production) changes occurring on the skin alter the dielectric constant of the bananas, which causes a frequency shift in the readings (**Figure 9b**). Day 9 of storage was confirmed as the full ripening day with the sensor. The same gold-silk RFID sensor tags were also used in the detection of cheese spoilage. Detection of spoilage was confirmed with the presence of pathogenic bacteria on the surface of cheese slices, as shown in **Figure 9c**. Lastly, the performance of the gold-silk RFID tags was tested in liquid milk samples to test bacterial spoilage. The changing relative permittivity measured by the sensor confirmed milk spoilage during storage (**Figure 9d**).

In another study, milk spoilage rates were determined with RFID sensor tags attached to the outer wall of two types of milk carton, those of fat-free milk and vitamin D-fortified whole milk (Potyrai et al. 2009, 2012). Similar to Tao et al.'s (2012) study, milk spoilage was monitored with dielectric constant changes occurring over time and compared to water samples as controls. RFID tags were successful in determining spoilage for 40 hours of storage as well as differentiating whole milk and fat-free milk spoilage profiles from each other.

Eom et al. (2014) developed a smart RFID tag sensor to monitor meat freshness and use-by dates. The RFID system was coupled with a temperature sensor, a humidity sensor, and a gas sensor to measure the environmental factors and ammonia gas produced during spoilage of the meat. Gas sensor results were used to estimate the meat freshness, and temperature and humidity readings

were used to estimate a food poisoning index (high freshness, medium freshness, low freshness, spoilage) for customers to decide whether it is safe to consume the product. The freshness of pork meat was tested with RFID sensors, and spoilage conditions were successfully analyzed with the measured temperature, humidity, and ammonia levels. The performance of the RFID sensors was also confirmed with parallel measurements done with e-nose sensors. Other RFID-based sensors are used to determine beef (Nguyen et al. 2013) or seafood (Potyrai et al. 2012) freshness levels.

RFID tags were designed to detect the maturation levels of Emmentaler-type Swiss cheese during ripening (Abdelnour et al. 2019). Two changes occurring during cheese ripening were used as measurement parameters: (a) cheese swelling due to carbon dioxide formation and (b) increase in pressure caused by gases that are emitted during deterioration in the plastic packaging. In the first sensor configuration, a stretchable cord was used that increased its resistance as the cheese increased in diameter and the cord stretched out. Measurements taken for 63 days of ripening showed that RFID tags placed outside the packaging materials could successfully measure the 3–4-cm volume increase in cheese products. In the second configuration, RFID tags with pressure sensors were placed inside the packaging materials and data were collected during 58 days of ripening. RFID tags were able to detect a complete pressure change of over 700 mBar during cheese ripening, proving successful monitoring of fermentation during maturation.

### 3. CONCLUSIONS

In this review, we summarized the recent studies that focused on the fabrication of biosensors for (a) detecting food hazards, such as allergens, toxins, contaminants, and pathogens; (b) assessment of food quality, safety, and content; and (c) efficient traceability of food products. We have categorized the food biosensors under four groups based on the most commonly used transducers in their design: optical, electrochemical, mechanical, and RFID-based transducers. Each biosensor group has unique applicability and advantages of its own.

Optical biosensors have the advantage of being the most nondestructive sensors, and measurements of harmful substances can be done from a distance because the light output can be captured by a noncontact detector. They both allow the choice of label-free and label-based detections, and they are the most advantageous to be used for on-site measurements because their configuration can be as simple as a color change on a disposable paper strip. The most common use of optical biosensors is found in food safety, where a lot of research is going on especially in the detection of pathogens, food spoilage bacteria, viruses, and pesticides.

Electrochemical biosensors are the most commonly used type of biosensors. They generally have higher sensitivities compared to other biosensors because the electrodes used in their design are capable of detecting the slightest changes in electrical output. Label-free detections are also possible with electrochemical biosensors. However, the electrode configuration does not make them the first choice when it comes to making on-site measurements, and the samples tested usually need to be discarded. Electrochemical biosensors have a wider range of food applications compared to other biosensors, food safety being the most commonly chosen area.

Mechanical biosensors have found less use than optical or electrochemical biosensors because of their complex and costly fabrication. Their mass-based detection principle allows label-free measurements and their nanoscales allow very low LODs. The most commonly used area of mechanical biosensors is microorganism detection, where single-cell detections are possible.

RFID-based sensors are mostly used for tracing food products and determining their quality, such as food freshness. Portable RFID devices and wireless technology make them the most easy-to-use sensors in every step of the food supply chain. This is probably why RFID-based sensors are almost the only type of sensor that has found industrial applications.

Despite the massive amount of research and development effort, food biosensors are sparsely used in the food industry. However, this review shows the great potential of biosensors to replace many of the currently used cumbersome and difficult detection techniques in the food industry. Especially with the developing nanotechnology methods, such as nanomachinery or nanoprinting, the sensitivity and selectivity of biosensors are tremendously increased. Specifically, with this increased sensitivity and selectivity, biosensors carry great potential to be the primary detection devices for point-of-care analyses in the future.

## DISCLOSURE STATEMENT

The authors are not aware of any affiliations, memberships, funding, or financial holdings that might be perceived as affecting the objectivity of this review.

## ACKNOWLEDGMENTS

This study was supported by USDA HATCH ILLU-698-364 and USDA NIFA-AFRI 2017-67017-26472 grants and Purdue Scholle Endowment funds (F.00093509.06.001). We would like to acknowledge Frederick Seitz Materials Research Laboratory Central Facilities at the University of Illinois, Birck Nanotechnology Center at Purdue University, and the Research Instrumentation Center at the Department of Chemistry at Purdue University for making the techniques available at a very low cost. We would like to thank Dr. Gang Logan Liu, Dr. Miko Cakmak, Dr. Lia Stanciu, Dr. Arun Bhunia, and Dr. Vladimir Shalaev for their valuable contributions.

## LITERATURE CITED

- Abdelnour A, Fonseca N, Rennane A, Kaddour D, Tedjini S. 2019. Design of RFID sensor tag for cheese quality monitoring. In *Proceedings of the 2019 IEEE MTT-S International Microwave Symposium*, pp. 290–92. Piscataway, NJ: IEEE
- Aghaei Z, Ghorani B, Emadzadeh B, Kakhodaee R, Tucker N. 2020. Protein-based halochromic electrospun nanosensor for monitoring trout fish freshness. *Food Control* 111:107065
- Aghoutane Y, Diouf A, Österlund L, Bouchikhi B, El Bari N. 2020. Development of a molecularly imprinted polymer electrochemical sensor and its application for sensitive detection and determination of malathion in olive fruits and oils. *Bioelectrochemistry* 132:107404
- Ansari S, Bozkurt F, Yazar G, Ryan V, Bhunia A, Kokini J. 2015. Probing the distribution of gliadin proteins in dough and baked bread using conjugated quantum dots as a labeling tool. *J. Cereal Sci.* 63:41–48
- Arlett JL, Myers EB, Roukes ML. 2011. Comparative advantages of mechanical biosensors. *Nat. Nanotechnol.* 6(4):203–15
- Baek SH, Park CY, Nguyen TP, Kim MW, Park JP, et al. 2020. Novel peptides functionalized gold nanoparticles decorated tungsten disulfide nanoflowers as the electrochemical sensing platforms for the norovirus in an oyster. *Food Control* 114:107225
- Bagheri N, Khataee A, Habibi B, Hassanzadeh J. 2018. Mimetic Ag nanoparticle/Zn-based MOF nanocomposite (AgNPs@ZnMOF) capped with molecularly imprinted polymer for the selective detection of patulin. *Talanta* 179:710–18
- Barber EA, Turasan H, Gezer PG, Devina D, Liu GL, Kokini J. 2019. Effect of plasticizing and crosslinking at room temperature on microstructure replication using soft lithography on zein films. *J. Food Eng.* 250:55–64
- Bashir R. 2004. BioMEMS: state-of-the-art in detection, opportunities and prospects. *Adv. Drug Deliv. Rev.* 56(11):1565–86
- Becker MM, Ribeiro EB, de Oliveira Marques PRB, Marty J-L, Nunes GS, Catanante G. 2019. Development of a highly sensitive xanthine oxidase-based biosensor for the determination of antioxidant capacity in Amazonian fruit samples. *Talanta* 204:626–32

- Bera MK, Mohapatra S. 2020. Ultrasensitive detection of glyphosate through effective photoelectron transfer between CdTe and chitosan derived carbon dot. *Colloids Surf. A* 596:124710
- Boisen A, Dohn S, Keller SS, Schmid S, Tenje M. 2011. Cantilever-like micromechanical sensors. *Rep. Prog. Phys.* 74(3):036101
- Bonilla JC, Bernal-Crespo V, Schaber JA, Bhunia AK, Kokini JL. 2019a. Simultaneous immunofluorescent imaging of gliadins, low molecular weight glutenins, and high molecular weight glutenins in wheat flour dough with antibody-quantum dot complexes. *Food Res. Int.* 120:776–83
- Bonilla JC, Bozkurt F, Ansari S, Sozer N, Kokini JL. 2016. Applications of quantum dots in food science and biology. *Trends Food Sci. Technol.* 53:75–89
- Bonilla JC, Erturk MY, Kokini JL. 2020a. Understanding the role of gluten subunits (LMW, HMW glutenins and gliadin) in the networking behavior of a weak soft wheat dough and a strong semolina wheat flour dough and the relationship with linear and non-linear rheology. *Food Hydrocoll.* 108:106002
- Bonilla JC, Erturk MY, Schaber JA, Kokini JL. 2020b. Distribution and function of LMW glutenins, HMW glutenins, and gliadins in wheat doughs analyzed with ‘in situ’ detection and quantitative imaging techniques. *J. Cereal Sci.* 93:102931
- Bonilla JC, Ryan V, Yazar G, Kokini JL, Bhunia AK. 2018. Conjugation of specifically developed antibodies for high- and low-molecular-weight glutenins with fluorescent quantum dots as a tool for their detection in wheat flour dough. *J. Agric. Food Chem.* 66(16):4259–66
- Bonilla JC, Schaber JA, Bhunia AK, Kokini JL. 2019b. Mixing dynamics and molecular interactions of HMW glutenins, LMW glutenins, and gliadins analyzed by fluorescent co-localization and protein network quantification. *J. Cereal Sci.* 89:102792
- Bozkurt F, Ansari S, Yau P, Yazar G, Ryan V, Kokini J. 2014. Distribution and location of ethanol soluble proteins (Osborne gliadin) as a function of mixing time in strong wheat flour dough using quantum dots as a labeling tool with confocal laser scanning microscopy. *Food Res. Int.* 66:279–88
- Brainina K, Tarasov A, Khamzina E, Stozhko N, Vidrevich M. 2020. Contact hybrid potentiometric method for on-site and in situ estimation of the antioxidant activity of fruits and vegetables. *Food Chem.* 309:125703
- Bunney J, Williamson S, Atkin D, Jeanneret M, Cazzolino D, Chapman J. 2017. The use of electrochemical biosensors in food analysis. *Curr. Res. Nutr. Food Sci. J.* 5(3):183–95
- Cai S, Li W, Xu P, Xia X, Yu H, et al. 2019. In situ construction of metal-organic framework (MOF) UiO-66 film on Parylene-patterned resonant microcantilever for trace organophosphorus molecules detection. *Analyst* 144(12):3729–35
- Chambers JP, Arulanandam BP, Matta LL, Weis A, Valdes JJ. 2008. Biosensor recognition elements. *Curr. Issues Mol. Biol.* 10(1–2):1–12
- Chen G-H, Chen W-Y, Yen Y-C, Wang C-W, Chang H-T, Chen C-F. 2014. Detection of mercury(II) ions using colorimetric gold nanoparticles on paper-based analytical devices. *Anal. Chem.* 86(14):6843–49
- Chen X, Bai X, Li H, Zhang B. 2015. Aptamer-based microcantilever array biosensor for detection of fumonisin B-1. *RSC Adv.* 5(45):35448–52
- Chen Y, Liu L, Xu L, Song S, Kuang H, et al. 2017. Gold immunochromatographic sensor for the rapid detection of twenty-six sulfonamides in foods. *Nano Res.* 10(8):2833–44
- Claussen JC, Franklin AD, Ul-Haque A, Porterfield DM, Fisher TS. 2009. Electrochemical biosensor of nanocube-augmented carbon nanotube networks. *ACS Nano.* 3(1):37–44
- Costa C, Antonucci F, Pallottino F, Aguzzi J, Sarriá D, Menesatti P. 2013. A review on agri-food supply chain traceability by means of RFID technology. *Food Bioprocess Technol.* 6(2):353–66
- Costa CAB, Grazhdan D, Fiutowski J, Nebling E, Blohm L, et al. 2020. Meat and fish freshness evaluation by functionalized cantilever-based biosensors. *Microsyst. Technol.* 26(3):867–71
- da Silva W, Ghica ME, Ajayi RF, Iwuoha EI, Brett CMA. 2019. Tyrosinase based amperometric biosensor for determination of tyramine in fermented food and beverages with gold nanoparticle doped poly(8-anilino-1-naphthalene sulphonic acid) modified electrode. *Food Chem.* 282:18–26
- Damborský P, Švitel J, Katrlík J. 2016. Optical biosensors. *Essays Biochem.* 60(1):91–100
- Dridi F, Marrakchi M, Gargouri M, Saulnier J, Jaffrezic-Renault N, Lagarde F. 2017. Nanomaterial-based electrochemical biosensors for food safety and quality assessment. In *Nanobiosensors*, ed. AM Grumezescu, pp. 167–204. Cambridge, MA: Academic

- Ebralidze II, Laschuk NO, Poisson J, Zenkina OV. 2019. Colorimetric sensors and sensor arrays. In *Nanomaterials Design for Sensing Applications*, ed. OV Zenkina, pp. 1–39. New York: Elsevier
- Eom K-H, Hyun K-H, Lin S, Kim J-W. 2014. The meat freshness monitoring system using the smart RFID tag. *Int. J. Distrib. Sens. Netw.* <https://doi.org/10.1155/2014/591812>
- Ercole C, Del Gallo M, Mosiello L, Baccella S, Lepidi A. 2003. *Escherichia coli* detection in vegetable food by a potentiometric biosensor. *Sens. Actuators B* 91(1):163–68
- Estrela P, Damborský P, Švitel J, Katrlík J. 2016. Optical biosensors. *Essays Biochem.* 60(1):91–100
- FDA. 2020. Survey data on acrylamide in food. *FDA*. <https://www.fda.gov/food/chemicals/survey-data-acrylamide-food>
- Gardner JW, Bartlett PN. 1994. A brief history of electronic noses. *Sens. Actuators B* 18(1):210–11
- Gezer PG, Hsiao A, Kokini JL, Liu GL. 2016a. Simultaneous transfer of noble metals and three-dimensional micro- and nanopatterns onto zein for fabrication of nanophotonic platforms. *J. Mater. Sci.* 51(8):3806–16
- Gezer PG, Liu GL, Kokini JL. 2016b. Detection of acrylamide using a biodegradable zein-based sensor with surface enhanced Raman spectroscopy. *Food Control* 68:7–13
- Gezer PG, Liu GL, Kokini JL. 2016c. Development of a biodegradable sensor platform from gold coated zein nanophotonic films to detect peanut allergen, Ara h1, using surface enhanced raman spectroscopy. *Talanta* 150:224–32
- Girigoswami K, Akhtar N. 2019. Nanobiosensors and fluorescence based biosensors: an overview. *Int. J. Nano Dimens.* 10(1):1–17
- Gonzalez Viejo C, Fuentes S, Godbole A, Widdicombe B, Unnithan RR. 2020. Development of a low-cost e-nose to assess aroma profiles: an artificial intelligence application to assess beer quality. *Sens. Actuators B* 308:127688
- Grieshaber D, MacKenzie R, Vörös J, Reimhult E. 2008. Electrochemical biosensors: sensor principles and architectures. *Sensors* 8(3):1400–58
- Grimm JB, Heckman LM, Lavis LD. 2013. The chemistry of small-molecule fluorogenic probes. In *Progress in Molecular Biology and Translational Science*, Vol. 113, ed. MC Morris, pp. 1–34. Cambridge, MA: Academic
- Guan J-G, Miao Y-Q, Zhang Q-J. 2004. Impedimetric biosensors. *J. Biosci. Bioeng.* 97(4):219–26
- Gupta A, Akin D, Bashir R. 2004. Detection of bacterial cells and antibodies using surface micromachined thin silicon cantilever resonators. *J. Vac. Sci. Technol. B* 22(6):2785–91
- Han S, Deng R, Xie X, Liu X. 2014. Enhancing luminescence in lanthanide-doped upconversion nanoparticles. *Angew. Chem. Int. Ed.* 53(44):11702–15
- He L, Chen T, Labuza TP. 2014. Recovery and quantitative detection of thiabendazole on apples using a surface swab capture method followed by surface-enhanced Raman spectroscopy. *Food Chem.* 148:42–46
- He L, Lamont E, Veeregowda B, Sreevatsan S, Haynes CL, et al. 2011. Aptamer-based surface-enhanced Raman scattering detection of ricin in liquid foods. *Chem. Sci.* 2(8):1579–82
- He L, Liu Y, Lin M, Mustapha A, Wang Y. 2008. Detecting single *Bacillus* spores by surface enhanced Raman spectroscopy. *Sens. Instrum. Food Qual. Saf.* 2(4):247
- Henao-Escobar W, del Torno-de Román L, Domínguez-Renedo O, Alonso-Lomillo MA, Arcos-Martínez MJ. 2016. Dual enzymatic biosensor for simultaneous amperometric determination of histamine and putrescine. *Food Chem.* 190:818–23
- Herrero JL, Lozano J, Santos JP, Suárez JI. 2016. On-line classification of pollutants in water using wireless portable electronic noses. *Chemosphere* 152:107–16
- Hua QT, Ruecha N, Hiruta Y, Citterio D. 2019. Disposable electrochemical biosensor based on surface-modified screen-printed electrodes for organophosphorus pesticide analysis. *Anal. Methods.* 11(27):3439–45
- Jia F, Barber E, Turasan H, Seo S, Dai R, et al. 2019. Detection of pyocyanin using a new biodegradable SERS biosensor fabricated using gold coated zein nanostructures further decorated with gold nanoparticles. *J. Agric. Food Chem.* 67(16):4603–10
- Jia Z, Shi C, Wang Y, Yang X, Zhang J, Ji Z. 2020. Nondestructive determination of salmon fillet freshness during storage at different temperatures by electronic nose system combined with radial basis function neural networks. *Int. J. Food Sci. Technol.* 55(5):2080–91

- Kamel AH, Amr AE-GE, Abdalla NS, El-Naggar M, Al-Omar MA, Almehezia AA. 2020. Modified screen-printed potentiometric sensors based on man-tailored biomimetics for diquat herbicide determination. *Int. J. Environ. Res. Public Health*. 17(4):1138
- Kaur I, Sharma M, Kaur S, Kaur A. 2020. Ultra-sensitive electrochemical sensors based on self-assembled chelating dithiol on gold electrode for trace level detection of copper(II) ions. *Sens. Actuators B* 312:127935
- Khan R, Ben Aissa S, Sherazi TA, Catanante G, Hayat A, Marty JL. 2019. Development of an impedimetric aptasensor for label free detection of patulin in apple juice. *Molecules* 24(6):1017
- Khemthongcharoen N, Wonglumsom W, Suppat A, Jaruwongrungrsee K, Tuantranont A, Promptnas C. 2015. Piezoresistive microcantilever-based DNA sensor for sensitive detection of pathogenic *Vibrio cholerae* O1 in food sample. *Biosens. Bioelectron.* 63:347–53
- Kumar P, Reinitz HW, Simunovic J, Sandeep KP, Franzon PD. 2009. Overview of RFID technology and its applications in the food industry. *J. Food Sci.* 74(8):R101–6
- Kumar S, Dilbaghi N, Barnela M, Bhanjana G, Kumar R. 2012. Biosensors as novel platforms for detection of food pathogens and allergens. *BioNanoScience* 2(4):196–217
- Lal S, Grady NK, Kundu J, Levin CS, Lassiter JB, Halas NJ. 2008. Tailoring plasmonic substrates for surface enhanced spectroscopies. *Chem. Soc. Rev.* 37(5):898–911
- Lamont EA, He L, Warriner K, Labuza TP, Sreevatsan S. 2011. A single DNA aptamer functions as a biosensor for ricin. *Analyst* 136(19):3884–95
- Li A, Tang L, Song D, Song S, Ma W, et al. 2016. A SERS-active sensor based on heterogeneous gold nanostar core-silver nanoparticle satellite assemblies for ultrasensitive detection of aflatoxinB1. *Nanoscale* 8(4):1873–78
- Li H, Ahmad W, Rong Y, Chen Q, Zuo M, et al. 2020. Designing an aptamer based magnetic and upconversion nanoparticles conjugated fluorescence sensor for screening *Escherichia coli* in food. *Food Control* 107:106761
- Li J, Zhou YX, Guo YX, Wang GY, Maier RRJ, et al. 2018. Label-free ferrule-top optical fiber micro-cantilever biosensor. *Sens. Actuators Phys.* 280:505–12
- Lin L, Wu X, Cui G, Song S, Kuang H, Xu C. 2020. Colloidal gold immunochromatographic strip assay for the detection of azaperone in pork and pork liver. *ACS Omega.* 5(3):1346–51
- Lin M, He L, Awika J, Yang L, Ledoux DR, et al. 2008. Detection of melamine in gluten, chicken feed, and processed foods using surface enhanced Raman spectroscopy and HPLC. *J. Food Sci.* 73(8):T129–34
- Liu N, Nie D, Tan Y, Zhao Z, Liao Y, et al. 2017. An ultrasensitive amperometric immunosensor for zearalenones based on oriented antibody immobilization on a glassy carbon electrode modified with MWC-NTs and AuPt nanoparticles. *Microchim. Acta.* 184(1):147–53
- Liu T, Zhang W, Yuwono M, Zhang M, Ueland M, et al. 2020. A data-driven meat freshness monitoring and evaluation method using rapid centroid estimation and hidden Markov models. *Sens. Actuators B* 311:127868
- Lobnik A, Urek SK, Turel M. 2012. Quantum dots based optical sensors. In *Diffusion in Solids and Liquids*, ed. A Ochsner, GE Murch, A Shokuhfar, J Delgado, pp. 682–89. Zurich: Trans Tech Publ.
- Luka G, Ahmadi A, Najjaran H, Alocilja E, DeRosa M, et al. 2015. Microfluidics integrated biosensors: a leading technology towards lab-on-a-chip and sensing applications. *Sensors* 15(12):30011–31
- Ma X, Turasan H, Jia F, Seo S, Wang Z, et al. 2020. A novel biodegradable ESERS (enhanced SERS) platform with deposition of Au, Ag and Au/Ag nanoparticles on gold coated zein nanophotonic structures for the detection of food analytes. *Vib. Spectrosc.* 106:103013
- Maher RC. 2012. SERS hot spots. In *Raman Spectroscopy for Nanomaterials Characterization*, ed. CSSR Kumar, pp. 215–60. Berlin: Springer
- Malvano F, Albanese D, Pilloton R, Di Matteo M. 2017. A new label-free impedimetric aptasensor for gluten detection. *Food Control* 79:200–6
- Malvano F, Pilloton R, Albanese D. 2020. Label-free impedimetric biosensors for the control of food safety: a review. *Int. J. Environ. Anal. Chem.* 100(4):468–91
- Mansouri M, Khalilzadeh B, Barzegari A, Shoeibi S, Isildak S, et al. 2020. Design a highly specific sequence for electrochemical evaluation of meat adulteration in cooked sausages. *Biosens. Bioelectron.* 150:111916



- Milovanovic M, Žeravik J, Obořil M, Pelcová M, Lacina K, et al. 2019. A novel method for classification of wine based on organic acids. *Food Chem.* 284:296–302
- Misun PM, Rothe J, Schmid YRF, Hierlemann A, Frey O. 2016. Multi-analyte biosensor interface for real-time monitoring of 3D microtissue spheroids in hanging-drop networks. *Microsyst. Nanoeng.* 2:16022
- Mohtar LG, Aranda P, Messina GA, Nazareno MA, Pereira SV, et al. 2019. Amperometric biosensor based on laccase immobilized onto a nanostructured screen-printed electrode for determination of polyphenols in propolis. *Microchem. J.* 144:13–18
- Morris MC. 2013. Introduction. In *Progress in Molecular Biology and Translational Science*, Vol. 113, ed. MC Morris, pp. xv–xviii. Cambridge, MA: Academic
- Narang J, Chauhan N, Singh A, Pundir CS. 2011. A nylon membrane based amperometric biosensor for polyphenol determination. *J. Mol. Catal. B* 72(3):276–81
- Narsaiah K, Jha SN, Bhardwaj R, Sharma R, Kumar R. 2012. Optical biosensors for food quality and safety assurance—a review. *J. Food Sci. Technol.* 49(4):383–406
- Nguyen SD, Pham TT, Blanc EF, Le NN, Dang CM, Tedjini S. 2013. Approach for quality detection of food by RFID-based wireless sensor tag. *Electron. Lett.* 49(25):1588–89
- Özcan ŞM, Sesal NC, Şener MK, Koca A. 2020. An alternative strategy to detect bacterial contamination in milk and water: a newly designed electrochemical biosensor. *Eur. Food Res. Technol.* 246(6):1317–24
- Pang S, Labuza TP, He L. 2014. Development of a single aptamer-based surface enhanced Raman scattering method for rapid detection of multiple pesticides. *Analyst* 139(8):1895–901
- Park K, Jang J, Irimia D, Sturgis J, Lee J, et al. 2008. ‘Living cantilever arrays’ for characterization of mass of single live cells in fluids. *Lab Chip* 8(7):1034–41
- Persaud K, Dodd G. 1982. Analysis of discrimination mechanisms in the mammalian olfactory system using a model nose. *Nature* 299(5881):352–55
- Potyrailo RA, Morris WG, Sivavec T, Tomlinson HW, Klensmeden S, Lindh K. 2009. RFID sensors based on ubiquitous passive 13.56-MHz RFID tags and complex impedance detection. *Wirel. Commun. Mob. Comput.* 9(10):1318–30
- Potyrailo RA, Nagraj N, Tang Z, Mondello FJ, Surman C, Morris W. 2012. Battery-free radio frequency identification (RFID) sensors for food quality and safety. *J. Agric. Food Chem.* 60(35):8535–43
- Ren W, Ballou DR, FitzGerald R, Irudayaraj J. 2019. Plasmonic enhancement in lateral flow sensors for improved sensing of *E. coli* O157:H7. *Biosens. Bioelectron.* 126:324–31
- Ronkainen NJ, Halsall HB, Heineman WR. 2010. Electrochemical biosensors. *Chem. Soc. Rev.* 39(5):1747–63
- Rouf TB, Diaz-Amaya S, Stanciu L, Kokini J. 2020. Application of corn zein as an anchoring molecule in a carbon nanotube enhanced electrochemical sensor for the detection of gliadin. *Food Control* 117:107350
- Ruiz-Garcia L, Lunadei L, Barreiro P, Robla I. 2009. A review of wireless sensor technologies and applications in agriculture and food industry: state of the art and current trends. *Sensors* 9(6):4728–50
- Rusinek R, Gancarz M, Nawrocka A. 2020. Application of an electronic nose with novel method for generation of smellprints for testing the suitability for consumption of wheat bread during 4-day storage. *LWT Food Sci. Technol.* 117:108665
- Sha T, Liu J, Sun M, Li L, Bai J, et al. 2019. Green and low-cost synthesis of nitrogen-doped graphene-like mesoporous nanosheets from the biomass waste of okara for the amperometric detection of vitamin C in real samples. *Talanta* 200:300–6
- Sharma A, Khan R, Catanante G, Sherazi TA, Bhand S, et al. 2018. Designed strategies for fluorescence-based biosensors for the detection of mycotoxins. *Toxins* 10(5):197
- Silva NFD, Almeida CMR, Magalhães JMCS, Gonçalves MP, Freire C, Delerue-Matos C. 2019. Development of a disposable paper-based potentiometric immunosensor for real-time detection of a foodborne pathogen. *Biosens. Bioelectron.* 141:111317
- Soylemez S, Goker S, Toppare L. 2019. A promising enzyme anchoring probe for selective ethanol sensing in beverages. *Int. J. Biol. Macromol.* 133:1228–35
- Sozer N, Kokini JL. 2014. Use of quantum nanodot crystals as imaging probes for cereal proteins. *Food Res. Int.* 57:142–51
- Sun X, Guan L, Shan X, Zhang Y, Li Z. 2012. Electrochemical detection of peanut allergen Ara h 1 using a sensitive DNA biosensor based on stem-loop probe. *J. Agric. Food Chem.* 60(44):10979–84

- Suni II. 2008. Impedance methods for electrochemical sensors using nanomaterials. *TrAC Trends Anal. Chem.* 27(7):604–11
- Tao H, Brenckle MA, Yang M, Zhang J, Liu M, et al. 2012. Silk-based conformal, adhesive, edible food sensors. *Adv. Mater.* 24(8):1067–72
- Thakur MS, Ragavan KV. 2013. Biosensors in food processing. *J. Food Sci. Technol.* 50(4):625–41
- Tian Y, Liang T, Zhu P, Chen Y, Chen W, et al. 2019. Label-free detection of *E. coli* O157:H7 DNA using light-addressable potentiometric sensors with highly oriented ZnO nanorod arrays. *Sensors* 19(24):5473
- Tria SA, Lopez-Ferber D, Gonzalez C, Bazin I, Guiseppi-Elie A. 2016. Microfabricated biosensor for the simultaneous amperometric and luminescence detection and monitoring of ochratoxin A. *Biosens. Bioelectron.* 79:835–42
- Turasan H, Cakmak M, Kokini J. 2019. Fabrication of zein-based electrospun nanofiber decorated with gold nanoparticles as a SERS platform. *J. Mater. Sci.* 54(12):8872–91
- Wang J, Jiang L, Chu Q, Ye J. 2010. Residue analysis of melamine in milk products by micellar electrokinetic capillary chromatography with amperometric detection. *Food Chem.* 121(1):215–19
- Wang L, Hu Q, Pei F, Mugambi MA, Yang W. 2020. Detection and identification of fungal growth on freeze-dried *Agaricus bisporus* using spectra and olfactory sensors. *J. Sci. Food Agric.* 100(7):3136–46
- Wang P, Li H, Hassan MM, Guo Z, Zhang Z-Z, Chen Q. 2019. Fabricating an acetylcholinesterase modulated UCNPs-Cu<sup>2+</sup> fluorescence biosensor for ultrasensitive detection of organophosphorus pesticides-diazinon in food. *J. Agric. Food Chem.* 67(14):4071–79
- Weston M, Kuchel RP, Ciftci M, Boyer C, Chandrawati R. 2020. A polydiacetylene-based colorimetric sensor as an active use-by date indicator for milk. *J. Colloid Interface Sci.* 572:31–38
- Wijaya W, Pang S, Labuza TP, He L. 2014. Rapid detection of acetamiprid in foods using surface-enhanced raman spectroscopy (SERS). *J. Food Sci.* 79(4):T743–47
- Wu H-Y, Choi CJ, Cunningham BT. 2012. Plasmonic nanogap-enhanced Raman scattering using a resonant nanodome array. *Small* 8(18):2878–85
- Wu Z, Xu E, Chughtai MFJ, Jin Z, Irudayaraj J. 2017. Highly sensitive fluorescence sensing of zearalenone using a novel aptasensor based on upconverting nanoparticles. *Food Chem.* 230:673–80
- Xu L, Yu X, Liu L, Zhang R. 2016. A novel method for qualitative analysis of edible oil oxidation using an electronic nose. *Food Chem.* 202:229–35
- Xu Y, Niu X, Zhang H, Xu L, Zhao S, et al. 2015. Switch-on fluorescence sensing of glutathione in food samples based on a graphitic carbon nitride quantum dot (g-CNQD)-Hg<sup>2+</sup> chemosensor. *J. Agric. Food Chem.* 63(6):1747–55
- Yagati AK, Chavan SG, Back C, Lee M-H, Min J. 2018. Label-free impedance sensing of aflatoxin B1 with polyaniline nanofibers/Au nanoparticle electrode array. *Sensors* 18(5):1320
- Yang T, Zhang Z, Zhao B, Hou R, Kinchla A, et al. 2016. Real-time and in situ monitoring of pesticide penetration in edible leaves by surface-enhanced Raman scattering mapping. *Anal. Chem.* 88(10):5243–50
- Yin M, Jing C, Li H, Deng Q, Wang S. 2020. Surface chemistry modified upconversion nanoparticles as fluorescent sensor array for discrimination of foodborne pathogenic bacteria. *J. Nanobiotechnol.* 18(1):41
- Yun Y, Pan M, Wang L, Li S, Wang Y, et al. 2019. Fabrication and evaluation of a label-free piezoelectric immunosensor for sensitive and selective detection of amantadine in foods of animal origin. *Anal. Bioanal. Chem.* 411(22):5745–53
- Zhang X, Liu Q, Chen Z, Zuo X. 2020. Colorimetric sensor array for accurate detection and identification of antioxidants based on metal ions as sensor receptors. *Talanta* 215:120935
- Zhu Y, Wu J, Han L, Wang X, Li W, et al. 2020. Nanozyme sensor arrays based on heteroatom-doped graphene for detecting pesticides. *Anal. Chem.* 92(11):7444–52